HYDROGEN BOND DYNAMICS IN ALCOHOL CLUSTERS

MARTIN A. SUHM

Institut für Physikalische Chemie, Universität Göttingen, 37077 Göttingen, Germany

CONTENTS

Advances in Chemical Physics, Volume 142, edited by Stuart A. Rice

I. INTRODUCTION

Alcohols are the conceptually simplest organic molecules that undergo classical hydrogen bonding. Given the enormous importance of hydrogen bonding in complex organic and biological matter [1, 2], it is imperative to understand its dynamics for such simple, yet realistic, model systems. By adding one molecule at a time, the evolution from single molecules to condensed phases can be mapped out in a molecular cluster approach [3]. In contrast to the more elementary, more abundant, but completely singular water system [4], alcohols can be tailored by modifying their molecular backbone [5]. This ''chemical'' dimension renders them particularly valuable for supramolecular design [6]. In terms of hydrogen bond topology, it is the reduced dimensionality which makes alcohols attractive. Compared to the complex three-dimensional network present in water, the propensity for ring and chain aggregation in alcohol clusters [7] provides an elementary starting point for the investigation of energy flow along a sequence of intermolecular interactions [8], with important applications in solution and neat liquid phases [9–11]. The coexistence of hydrophobic and hydrophilic domains also leads to interesting surface effects [12] and microstructure in liquid alcohols [13], quite in contrast to water. Alcohols are clearly among the most elementary and longest known [14] protagonists in gas-phase supramolecular chemistry [15].

A dedicated review on hydrogen bonding in isolated alcohol clusters bridging methanol on one side [16] and sugars on the other [17] appears timely. In 1996, there were about 12 citations to publications including the keywords jet*, hydrogen*, and alcohol*, according to the Web of Science [18]. In 2006, there were more than 200. In view of several available reviews on aromatic systems [19–21], the focus will be on the less-studied aliphatic alcohols, which come closer to being amphiphilic models. For solutions, where the first studies using nuclear magnetic resonance (NMR) and infrared (IR) spectroscopy date back more than half a century, a recent review concentrating on sterical

hindrance effects is available [22]. In the solid [23], packing effects always compete with the intrinsic properties of the isolated or cooperative hydrogen bonds. While clusters are also postulated as highly fluxional units in the supercritical state [24, 25] and in solution [26], their detailed understanding rests on a proper characterization at lower temperatures. At room temperature, the cluster concentration in the vapor phase of alcohols is fairly low and thermal excitation still makes an interpretation of the spectra difficult [27]. Therefore, the present review concentrates on cold molecular aggregates, which are most conveniently produced and studied in adiabatic gas expansions or jets [28]. The ultimate goal is to use the detailed insights gained in such low-temperature gas-phase studies to better understand the hydrogen bond and conformational behavior in the liquid state [29, 30].

After raising a selection of topical issues in this field and briefly introducing some spectroscopic and numerical techniques to probe the hydrogen bond dynamics, recent results for alcohol clusters are presented in order of increasing complexity. They are followed by some general conclusions and an outlook on future research goals.

II. ISSUES

Among the wealth of issues relevant to hydrogen bonding in alcohol clusters, this review will focus on aspects related to hydrogen bond patterns and on the dynamical implications over a wide range of time scales. Some key questions connected to these aspects will be formulated.

A. Structures and Topologies

O—H$\cdots$O hydrogen bonds have a strong preference for a nearly linear arrangement. Furthermore, electrostatic forces or lone electron pair considerations direct the hydrogen that is attached to the accepting oxygen into an approximately tetrahedral angle with respect to the hydrogen bond. The tetrahedral lone-pair picture has recently been debated [31], based on electron density maps and earlier structural evidence on poly-alcohols [32]. While there is certainly significant acceptor potential in the region between the two lone pairs, the two studies [31, 32] may be biased in overestimating it slightly. Pauli repulsion will have to be included in the recent study [31] and distortions due to the optimization of multiple hydrogen bonds and steric constraints in the solid state have to be considered in the earlier analysis [32]. When taken into account, both effects are likely to recover a certain tetrahedral preference in isolated hydrogen bonds. This may or may not be cast into a lone-pair picture. At least it is an extremely useful ordering principle for alcohol cluster structures, which does not rule out exceptions.

In line with this, alcohols form unsymmetric dimers with well-separated donor and acceptor roles [33] and a more or less pronounced preference for one of the acceptor lone pairs, depending on secondary interactions (see Fig. 1). For trimers, the option to form a ring with three hydrogen bonds usually wins over the hydrogen bond strain and over steric repulsion between the alkyl groups which this induces. However, the open-chain structure with two unstrained hydrogen bonds is not too far in energy and always should be considered for vibrationally excited clusters [34] and whenever secondary interactions come into play [35, 36]. Furthermore, trimer formation can be suppressed at least at elevated temperatures [37], if the alkyl chain becomes too bulky. For the tetramer, a cyclic structure involves less strain and less sterical hindrance than in the trimer and is thus particularly attractive (Fig. 1). The alkyl groups can alternate between positions above and below the hydrogen bond plane and better avoid each other, if they are too big. Again, this alternation can also be interpreted as being due to a lone-pair preference. In terms of pure repulsion, a planar arrangement of all heavy atoms is indeed competitive, if the alkyl group

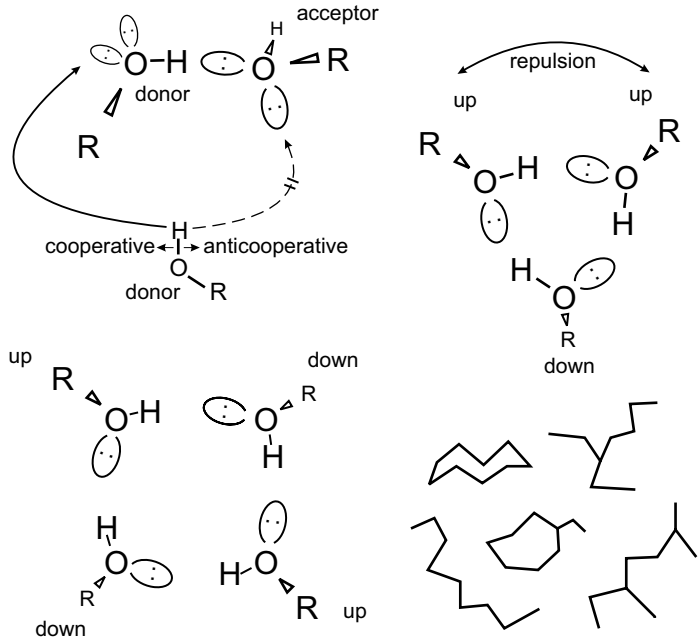

Figure 1. Illustration of lone-electron-pair preferences in alcohol dimers, cooperative and anticooperative binding sites for a third monomer, ring strain and steric repulsion in alcohol trimers, alternation of residues in alcohol tetramers, and chain, branch, and cyclic hydrogen bond topologies in larger clusters.

is not too big. Rings with homodromic hydrogen bond patterns remain energetically attractive for larger clusters [38], but the entropic advantage of chain structures, where the terminal alcohol molecules only form single strong hydrogen bonds, and branched topologies, where alcohol molecules serve as double acceptors, tends to grow. Chain topologies can reduce steric congestion by forming helical structures, whereas branching tends to be more sterically demanding. Isomerism is therefore an important issue beyond a cluster size $n = 4$ [39] and possibly even before. In the solid, infinite chains and helices are often realized for simple alcohols [40], but cyclic structures are also conceivable [41] and quite abundant for bulky species [7, 42–44]. The structure of liquid alcohols is heavily debated [45]. Entropy arguments would predict winding chains of variable length to be quite important. The missing hydrogen bond compared to cyclic clusters can be partly compensated by the polar environment and by branching points. A finite cluster model of liquid alcohols [45] will necessarily be biased toward small clusters, closed rings, and compact structures, because it cannot reproduce the dramatic increase of conformational and topological entropy in extended flexible chains and dynamical network structures. Nevertheless, a detailed characterization of small clusters can bring us closer to a structural understanding of liquid alcohols.

The basic aggregation pattern in alcohol clusters can of course be influenced in any desired direction by the design of the alkyl group, a feature that makes alcohols attractive in molecular recognition studies. Molecular additives can further modify the topological preferences. By offering a pure hydrogen bond acceptor group such as an ether, terminated chain structures can be favored over rings [46]. By adding a local or global charge, major disruptions of the ring topology are possible, because charge coordination competes with the hydrogen bond network [47, 48]. However, the fundamental preference of alcohol clusters to form hydrogen-bonded ring patterns is never lost completely and reappears whenever other constraints start to relax.

B. Energetics

Unfortunately, not many techniques allow us to probe the binding energy of a hydrogen-bonded complex directly [20, 49–51]. With very few exceptions [52, 53], they are restricted to aromatic (π-) systems, where the intrinsic strength of a single alcoholic hydrogen bond is typically superimposed [54] and may even be overwhelmed [55] by π-interactions. Therefore, one often has to rely on quantum chemical sources for energy information [56, 57]. It is essential to calibrate these techniques against the few available experimental benchmark data, such as for methanol dimer [52], phenol–methanol [20], or 1-naphthol complexes [51]. Relative energy orders of isomers are even more important [50] and can sometimes be obtained by jet relaxation studies [58]. The strength of a hydrogen bond can be influenced by introducing electron-donating and electron-withdrawing alkyl

groups. Quite naturally, the hydrogen bond donor quality increases for electronegative substituents, whereas the acceptor quality decreases. For homodimers—that is, complexes built from identical subunits—the two influences compete with each other. Furthermore, the organic substituents can undergo their own intermolecular interactions, either among themselves or with the functional units of the O—H$\cdots$O hydrogen bond. Therefore, cluster binding energies are measures of the total interaction between the interacting molecules, which may or may not be dominated by a single classical hydrogen bond interaction. Donor–acceptor roles can become quite intricate in multifunctional systems [59]. This is another important motivation for studying the simplest prototype systems, where any secondary interactions are minimized.

C. Cooperativity

Another factor that influences the aggregation pattern and energetics of alcohol clusters is cooperativity [60]. Once a molecule engages as a hydrogen bond donor, it automatically becomes a better acceptor and *vice versa* due to the polarization of the O—H bond. This favors chain-like and even more cyclic topologies over branched networks of hydrogen bonds [61]. The latter are less stable, because two or more molecules must compete for the electron density at the acceptor oxygen (Fig. 1). It is more favorable for the third molecule to extend the polarization chain of the other two, rather than to interrupt it. The prototype system for this is hydrogen fluoride [62], which, more so than the reactive OH radical [63], may serve as the topological parent compound for alcohol aggregation. Its pronounced hierarchy of interactions (strong 1-D aggregation via cooperative hydrogen bonds, weak 3-D aggregation via dispersive forces) can be systematically attenuated by increasing the size of the alkyl group. This hierarchy is responsible for cluster formation in alcohol vapor even under thermodynamic equilibrium conditions [14, 64, 65].

Although cooperative effects are sometimes invoked whenever a property (such as a hydrogen bond length) changes from the dimer to larger aggregates [66], a many-body decomposition approach can uncover non-pairwise additive effects more rigorously [67]. The natural cluster size to study cooperativity is a trimer. The total energy of a trimer E_{ABC} can be decomposed into monomer energies E_A, E_B, E_C, pair interaction terms $V_{AB} = E_{AB} - E_A - E_B$, $V_{AC} = E_{AC} - E_A - E_C$, $V_{BC} = E_{BC} - E_B - E_C$, and a three-body interaction

$$V_{ABC} = E_{ABC} - E_{AB} - E_{AC} - E_{BC} + E_A + E_B + E_C$$

such that

$$E_{ABC} = E_A + E_B + E_C + V_{AB} + V_{AC} + V_{BC} + V_{ABC}$$

Only the effects of the three-body interaction term V_{ABC} are truly cooperative effects in a trimer, although properties may of course also change with cluster size in a strictly pairwise additive model, where $V_{ABC} = 0$. The formalism may easily be extended to larger clusters and indeed three-body effects tend to be more important in larger clusters than in trimers [68].

For chain-like or cyclic hydrogen bond patterns between three alcohol molecules A, B, and C, V_{ABC} is usually negative (attractive). If molecule B acts as an acceptor for both A and C, V_{ABC} is typically repulsive (positive), because A and C compete for the electron density at B [61]. This anti-cooperativity provides the main explanation why branching of hydrogen-bonded chains is discouraged in alcohols.

D. Hydrogen Bond Isomerism and Conformational Isomerism

For the reasons outlined above, hydrogen bond isomerism in alcohols is less pronounced than it might be on statistical grounds, considering that every acceptor oxygen offers a choice between two lone electron pairs. For ring topologies, there are of course different ways of arranging the alkyl groups already in the trimer and different ways of puckering the $(-OH)_n$ ring, starting with the tetramer or pentamer. Like isomerism within the alkyl chain [69], these are conformational choices that leave the classical hydrogen bond pattern intact. Hydrogen bond isomerism is less abundant. Lasso structures [39], in which double acceptor alcohol units come into play, only become competitive when the ring strain has leveled off—that is, for $n \geq 4$. The simple reason is that any molecule that is taken out of the ring makes the cycle smaller and increases ring strain. This penalty adds to the anti-cooperative effect present in double-acceptor centers. Open-chain structures are possibly competitive in small, highly strained clusters and become asymptotically equivalent to rings for $n \rightarrow \infty$. The best way to stabilize them for intermediate cluster sizes appears to be the introduction of secondary interactions in the alkyl group. Such a secondary stabilization can be an aromatic substituent [35].

When mixed clusters of alcohols are formed, the issue of donor–acceptor isomerism comes into play [58]. Both alcohols can act as donors and acceptors, but the difference between their donor (Q_D) and acceptor (Q_A) qualities ($Q_D - Q_A$) will not be the same. The molecule that features the smaller difference will preferentially act as an acceptor. The molecule that has the larger difference will prefer the donor position. If the roles are interchanged, the hydrogen bond strength of the complex decreases, but the structure may still represent a local minimum on the potential energy hypersurface. The determination of donor and acceptor qualities in hydrogen-bonded clusters is not straightforward. Energetic quantities such as binding energies are difficult to attribute to single interaction sites. Vibrational red shifts of the O—H stretching fundamental may be more suitable parameters to analyze the donor–acceptor

preference [58], because they closely correlate to hydrogen bond length and strength [70]. Furthermore, they are experimentally more easily accessible.

E. O—H Stretching Dynamics

The infrared (IR) spectrum provides some of the most clear-cut observables for hydrogen bonding phenomena. Alcohol clusters have been studied in most detail in the O—H stretching fundamental range. The reasons for this are both technical and scientific. Tunable IR lasers have traditionally been versatile and powerful in the 3-μm window. The effects of hydrogen bonding are also particularly pronounced in this range, as was recognized long ago [71]. Cooperativity and decreasing ring strain induce progressive bathochromic shifts with cluster size [16, 35]. The square of the O—H stretching transition dipole moment, responsible for IR activity, can be orders of magnitude larger in hydrogen-bonded clusters than in the alcohol monomer. Therefore, even in the absence of size-selectivity and sensitive laser sources, alcohol clusters can be detected and characterized by their O—H stretching signature [65].

The bathochromic shift or red shift of the O—H oscillator is a sensitive measure of hydrogen bond strength. Its accurate modeling is quite sophisticated, but simple approaches often profit from favorable error compensation [72]. Furthermore, the frequency of an O—H oscillator correlates more or less linearly with the length of the O—H bond, with a red shift of about $14\,\mathrm{cm}^{-1}$ for a bond length extension by 0.001 Å [63]. In larger clusters, the intrinsic red shift of the individual oscillators is superimposed by coupling effects among the originally degenerate oscillators of the individual alcohol monomers, the so-called Davydov couplings [16]. The strongest red shift is observed for concerted in-phase O—H stretching motion of all members of the hydrogen bond cycle. This is an early indicator for concerted hydrogen transfer between the molecules [73], in which the hydrogen-bonded protons switch their chemical bond partners in a cyclic way. The result is an equivalent hydrogen bond pattern running in the opposite direction. The pronounced red shift also reflects cooperativity, because a stretched O—H bond has an increased dipole moment, which enhances the intermolecular interaction.

Infrared enhancement in the O—H stretching fundamental upon hydrogen bond formation can be large, but may be smaller than predicted by traditional quantum chemistry methods [74]. There are few ways to experimentally determine absolute infrared enhancements by hydrogen bond formation [74], because the experimental number density of the clusters usually remains unknown. Instead, theoretical band strengths are often used to estimate the cluster number density [75]. The situation is more favorable if a cluster contains two or more nonequivalent O—H groups. In such a case, the intensity ratio between these groups can be determined by direct absorption methods [30, 76]. As a rule, Raman scattering cross sections are less sensitive to hydrogen bonding [16] but show similar qualitative trends.

The splitting patterns of the degenerate O—H oscillators upon cluster formation [77] can be described by a simple model, which is inspired by Hückel molecular orbital theory [16, 78]. These Davydov splittings reflect a periodic flow of energy among the coupled oscillators. For trimers, its period T is roughly related to the coupling constant W (in cm^{-1}) involved, according to

$$T \approx \frac{1}{3cW}$$

where c is the speed of light. Note that the dissipative formula for the lifetime τ

$$\tau \approx \frac{1}{2\pi cW}$$

has also been invoked in this context [78]. It agrees quite closely with the half-period of the oscillation. There are usually further, slower dissipative processes, by which the energy deposited in the O—H stretching manifold is redistributed within the alcohol molecules and into the hydrogen bond [21]. If these IVR processes are sufficiently fast and the density of coupling states is high enough, they can be detected as a contribution to the linewidth of the cluster O—H stretching band [16]. In any case, the two time–wavenumber relationships listed above are useful qualitative and semiquantitative concepts to translate spectral features into temporal evolutions of a localized wavepacket. For monomers and dimers, where the energy dissipation out of a locally excited O—H oscillator is relatively slow, IVR usually has to be detected by time-resolved experiments [21], which can provide further insights into the sequential mechanism.

The Davydov coupling constants W may be studied as a function of cluster geometry, cluster size, isotope composition, and alkyl group substitution [16]. They contain valuable information about the nature of the hydrogen bond interaction in alcohol clusters. The mechanism by which the Davydov couplings between initially degenerate O—H oscillators arises may be described in different ways. One may interpret it as a through-hydrogen-bond process, similar to classical oscillator coupling through chemical bonds. At the other end, one may interpret it as a purely through-space long-range coupling of the oscillating dipoles. Considering that hydrogen bonds between alcohols are dominated by dipole–dipole interactions, an excitonic dipole–dipole model appears to be adequate [78]. The coupling constant can then be estimated from the geometry and transition dipole moment of the cluster [78].

F. Isotope and Overtone Effects

A characteristic feature of hydride stretches in general [79] and the O—H oscillator in alcohols in particular [80] is its frequency isolation from other

degrees of freedom. This is an important cause for the relatively slow energy flow out of the O–H stretching state, and it invites reduced dimensionality treatments. Even at the harmonic level, this feature can be exploited to predict hydrogen-bond-induced red shifts in dimers, where Davydov couplings are small due to the mismatch of zeroth-order frequencies [80]. Beyond the harmonic approximation, the localization of the O–H stretching manifold invites experimental overtone studies [81–83] to extract anharmonicity constants and effective harmonic frequencies, which can be directly compared to theoretical predictions [16]. This works well for alcohol monomers, whereas for clusters the dramatic hydrogen-bond-induced intensity enhancement is lost in the overtone range due to a cancellation of electrical and mechanical anharmonicity contributions [84, 85] (see Fig. 2). Therefore, overtone vibrations of isolated hydrogen-bonded clusters

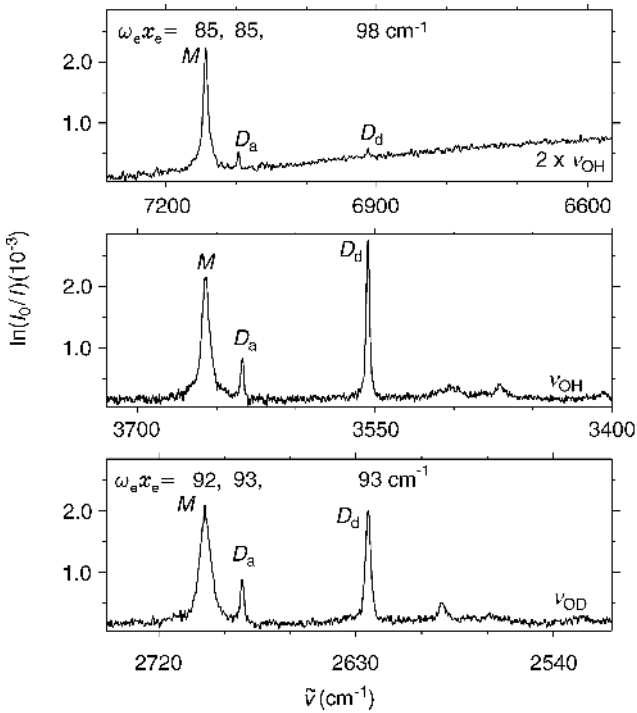

Figure 2. Extraction of anharmonicity constants $\omega_e x_e$ from the comparison of fundamental OH stretching spectra (**center**) with overtone spectra (**top**) and OD spectra (**bottom**) for the case of jet-cooled trifluoroethanol (M) and its most stable dimer conformation, which features a hydrogen bond donor stretching band (D_d) and an acceptor stretching band (D_a). The deuteration analysis yields slightly different constants than the overtone approach and underestimates the hydrogen bond effect on donor stretching modes [89].

are rarely observed [86], whereas they have been discussed in condensed phases [87] and have been important in the early days of hydrogen bond spectroscopy [71]. Recently, an alternative approach to O—H anharmonicity constants based on deuteration effects on the spectrum has been proposed [16, 88]. It is not as accurate as the overtone approach, because mode mixing is more likely for OD stretching modes and the constants are quite sensitive to this mixing [16]. However, it has provided first insights into the evolution of anharmonicity constants with cluster size. For methanol, it was shown in this way that dimerization leaves anharmonicity fairly unaffected, whereas anharmonic effects increase in the cyclic clusters [16]. This explains in part why harmonic predictions of bathochromic dimer shifts have been so successful in the past. However, very recent overtone measurements in supersonic jets [89] (see Fig. 2) indicate that the deuteration approach may indeed be of limited accuracy for the donor vibration in alcohol dimers.

Deuteration can also strengthen hydrogen bonds [90–92]. This is a zero-point energy effect. The high-frequency libration and torsion modes of the O—H group [93] decrease in energy, when the hydrogen atom is replaced by deuterium. In the monomers, the corresponding modes either have no (in the case of external rotations) or only little (in the case of internal rotations) zero-point energy. Therefore, the torsional isotope effect is much smaller for monomers. The net effect is an increase in dimer binding energy upon deuteration. There is a counteracting effect from the O—H stretching mode itself. Due to the red shift in the complex, its zero point energy is smaller in the hydrogen-bonded form than in the isolated molecule. Therefore, the effect of deuteration is larger in the monomer than in the cluster. For hydrogen bonds between alcohol molecules, this counteracting effect is usually smaller than the librational contribution. As a net effect, deuteration strengthens the hydrogen bonds in alcohol clusters.

G. C—O and C—H Stretching Dynamics

Although it is only a secondary effect, the influence of hydrogen bonding on the C—O stretching dynamics has received a lot of attention [94, 95]. This also has technical reasons, because the C—O stretching modes fall into the CO_2 laser range for several alcohols. Size selectivity is usually needed, because the contributions from different small clusters tend to overlap [96]. If available, structural details can be extracted from the coupling of the oscillators located on the individual monomers [94, 97, 98]. However, the C—O stretching mode is less isolated from other normal vibrations than the O—H stretching mode. Unusual evolutions of its frequency with cluster size or aggregation state may thus be due to mode mixings [65].

Even the dynamics of C—H stretching modes can reflect the hydrogen bond status of alcohol molecules [99, 100], in particular the local hydrogen bond

topology involved. Because the effects are considerably smaller than the O—H shifts and the monomer tends to dominate supersonic jet expansions, size-selective techniques are typically required to detect such spectroscopic cluster signatures. In favorable cases [30], cluster C—H absorptions can also be detected by direct absorption techniques on the slope of the dominant monomer bands.

H. Torsional Dynamics

A primary effect of hydrogen bonding is observed for the torsional dynamics of the O—H group. Torsion is orthogonal to the C—O—H bending mode and can be described as either (a) a hindered rotation of the entire alcohol molecule out of the hydrogen bond constraint or (b) a twisting motion around the C—O bond within the monomer. In the first case, the alkyl group moves in a conrotatory way with respect to the O—H group, whereas its motion is disrotatory in the second case. As a third possibility, the torsional motion in the cluster may be decoupled from the alkyl group motion, corresponding to a mixture of the monomer rotation and monomer torsion limits (see Fig. 3).

Torsion around C—C and C—O bonds connects different alcohol isomers. The analysis of interactions between torsional states which are concentrated in different torsional wells can provide important information on energy differences between conformations [101, 102]. Conformational isomerism in alcohols is so subtle that it cannot be easily separated from intermolecular influences in

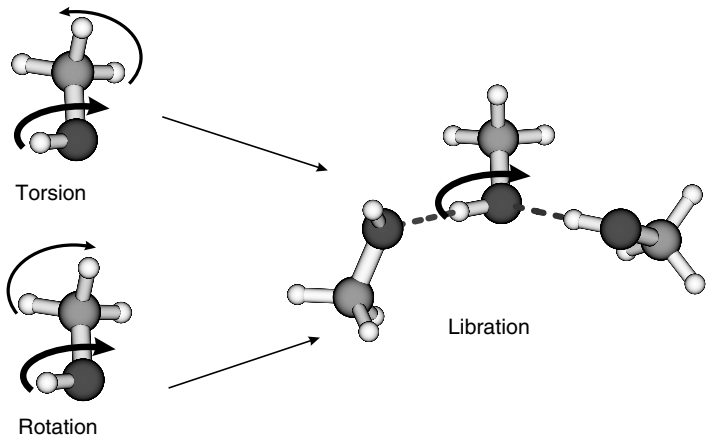

Figure 3. Librational OH modes in hydrogen-bonded alcohol clusters may be correlated with overall rotation (**bottom left**) and torsion (**top left**) of the monomer (illustrated for methanol), but methyl rotation is actually decoupled from OH torsion by hydrogen bonding. Note that the wavenumbers of monomer rotation ($\approx 4\,\mathrm{cm}^{-1}$) and torsion ($\approx 280\,\mathrm{cm}^{-1}$) are much lower than that of the cluster libration ($\approx 600\,\mathrm{cm}^{-1}$) [93].

condensed phases. Even the delicate interactions in rare gas matrices can overturn the intrinsic preference of the isolated molecule or molecular pair [80, 103]. Therefore low-temperature vacuum-isolated molecules are imperative in this field, if a reliable characterization of the unperturbed energy sequence of torsional isomers is sought. On the other hand, laser-induced torsional isomerization processes are much easier to study in cryogenic matrices [103, 104]. A deeper understanding of the dynamics among such torsional states can also contribute to the design of Brownian molecular machines [105].

I. Tunneling Dynamics

Several motions in alcohol clusters involve barriers that may be overcome by tunneling rather than by classical over-the-barrier motion. The concerted proton exchange mode between different alcohol molecules has already been mentioned and still remains to be detected in the O—H stretching spectrum of methanol tetramer, where it should be accelerated compared to the vibrational ground state [106]. Methyl torsions in the alkyl groups [107] also belong to this category and may be accelerated or decelerated by the hydrogen bond interaction.

Heavy atom tunneling of entire alkyl groups between the different sides of the hydrogen bonded ring plane is much less likely even for methanol, in contrast to the analogous but lighter water case [108]. These motions correspond to hindered rotation of the monomer and are slowed down considerably in the complex due to the librational constraints.

Finally, there can be rather large torsional tunneling splittings due to O—H torsion in the monomers (see the previous section), which are likely to be quenched almost completely by the intermolecular hydrogen bond. These tunneling processes in the monomers can themselves be affected by weaker intramolecular hydrogen bond interactions, such as C—H$\cdots$O contacts.

J. Chirality Recognition

Chirality or handedness is an important aspect for most organic molecules. In the case of alcohols, chirality is usually introduced by chemically or isotopically [109] different substituents at the α-C or a more distant site in the alkyl backbone. When two chiral molecules interact via alcoholic hydrogen bonds, their relative chirality will influence the interaction energy and the vibrational spectrum. This is an intermolecular variant of diastereoisomerism [110]. Dimers formed by two monomers of the same handedness are distinguishable from those of opposite handedness in the case of two constitutionally identical monomers. Beyond this special case, which has been denoted as a ''molecular handshake'' [111], chirality recognition may of course also occur between two different chiral alcohols [112, 113], where some convention [114] has to be used to define like and unlike partners. Depending on how close the chirality centers are to the O—H groups and how well the organic rests can accommodate the hydrogen bond

constraint, the observed differences between the two diastereomers may be more or less pronounced. For dimers of monofunctional alcohols, which are held together by nothing but one strong contact, only small differences are expected and are indeed found in the vibrational spectrum [115], whereas the differences in the UV spectrum are larger [112]. In the room temperature liquid, the differences are usually negligible in such a case [116]. Microwave spectroscopy is particularly well-suited to detect structural and spectral discrepancies between the two kinds of molecular pairs [117]. It is sensitive to the more subtle dispersion- and Pauli repulsion-like secondary interactions that convey the chirality information in the case of a single hydrogen bond contact [54]. In addition to optical spectroscopy, mass-spectrometric techniques are also useful to unravel chirality recognition effects in the gas phase [118].

One may use the stronger term *chirality discrimination* when a substantial suppression of one intermolecular diastereomer with respect to the other occurs. This requires multiple strong interactions between the two molecular units and therefore more than simple monofunctional alcohols. Some examples where one of the molecules involved is a chiral alkanol are reported in Refs. 112 and 119–121. Pronounced cases of higher-order chirality discrimination have been observed in clusters of hydroxyesters such as methyl lactate tetramers [122] and in protonated serine octamers [15, 123, 124]. The presence of an alcohol functionality appears to be favorable for accentuated chirality discrimination phenomena even in these complex systems [113, 123, 125, 126]. Because the border between chirality recognition and discrimination is quite undefined, it is suggested that the two may be used synonymously whenever both molecular partners are permanently chiral [127].

Even achiral alcohols may be involved in chirality recognition events by switching between labile enantiomeric conformations, depending on the permanent handedness of the binding partner. An example of such a *chirality induction* event involves the interaction of ethanol with a permanently chiral ether [128] and is illustrated in Fig. 4. Again, the chirality recognition is so weak that microwave spectroscopy is typically required to disentangle the different variants. Chirality induction is very important in organic synthesis, where chiral catalysts are used to favor the formation of one enantiomer over the other. An intramolecular variant, where the permanently chiral center of a chlorinated alcohol leads to a helicity preference in the intramolecular hydrogen bond conformation, was also studied by microwave spectroscopy [129].

If both alcohol monomers forming a dimer are on average achiral, one may still have *chirality synchronization* events, where the two monomers match their transient chiral conformations when they bind to each other. A particularly simple example is that of ethanol dimer, where the lowest-energy conformer involves two gauche monomers of the same helicity [80, 91]. However, the energy difference to other conformers is so small that efficient isomerizing collisions in a supersonic jet expansion are required to favor the lowest-energy form over the others. A more

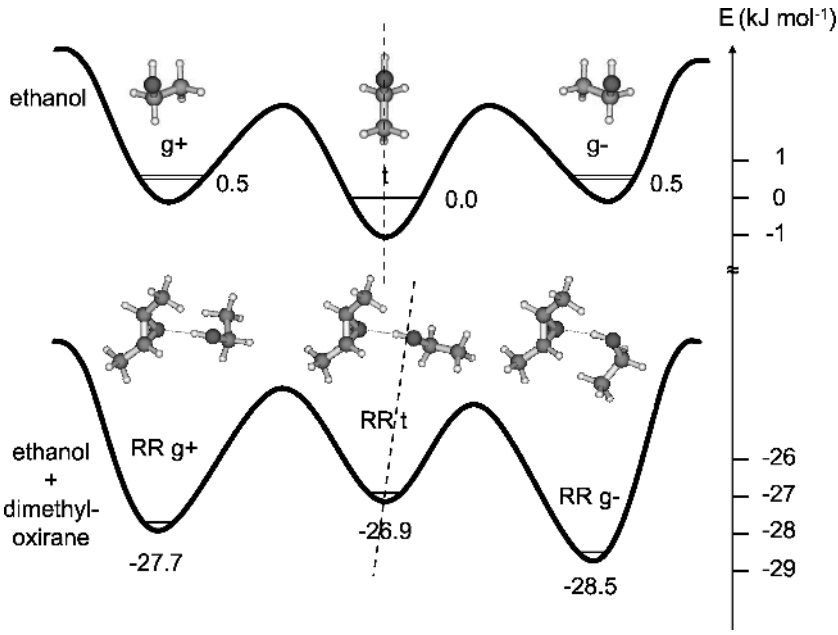

Figure 4. Symmetry breaking of the ethanol torsion potential (**top**, two gauche and one trans conformation) by interaction with a chiral acceptor molecule (dimethyl oxirane, **bottom**), in this case RR *trans*-2,3-dimethyloxirane [128]. Note that trans ethanol is less stable in the complex and that the two gauche (g) forms differ in energy.

pronounced example for chirality synchronization was found in trifluoroethanol [30, 76]. Here, the energy difference between a homoconformational and a heteroconformational dimer is predicted to be small, but they have a different hydrogen bond topology and only one of them is formed in significant amounts in a jet expansion [30, 76]. The intermediate case of fluoroethanol shows evidence for chirality recognition among the four dimer conformations that are observed in the spectrum, but no substantial chirality synchronization [130]. Chirality recognition phenomena in clusters involving no, one, two, or more permanently chiral constituents have recently been summarized [127].

K. Cation Solvation

Alcohols are important solvents for ions, and the study of solute–solvent clusters promises to provide insights into the solvation process. The solvation of protons by methanol [47], ethanol [131], and higher alcohols [132] has been studied in detail and leads to interesting hydrogen bond topologies [133]. Solvation of larger cations by alcohol molecules has been investigated for many years and may help in understanding the essentials of ion–water interactions [134].

L. Anion Solvation

Anion solvation in alcohol clusters has been studied extensively (see Refs. 135 and 136 and references cited therein). Among the anions that can be solvated by alcohols, the free electron is certainly the most exotic one. It can be attached to neutral alcohol clusters [137], or a sodium atom picked up by the cluster may dissociate into a sodium cation and a more or less solvated electron [48]. Solvation of the electron by alcohols may help in understanding the classical solvent ammonia and the more related and reactive solvent water [138]. By studying molecules with amine and alcohol functionalities [139] one may hope to unravel the essential differences between O- and N-solvents. One should note that dissociative electron attachment processes become more facile with an increasing number of O—H groups in the molecule [140].

III. EXPERIMENTAL METHODS

As became obvious in the preceding section, progress in understanding alcohol clusters very much depends on the ability to generate these clusters in supersonic jet expansions or in other variants of low temperature isolation and to detect their dynamics via spectroscopic methods. Therefore, some important spectroscopic tools employed in this field shall be summarized, with focus on the alcoholic systems that have been addressed by them. Solution [22, 26, 141, 142] and supercritical [24–26] state techniques will not be covered systematically.

A. Microwave Spectroscopy

Microwave spectroscopy is probably the ultimate tool to study small alcohol clusters in vacuum isolation. With the help of isotope substitution and auxiliary quantum chemical calculations, it provides structural insights and quantitative bond parameters for alcohol clusters [117, 143]. The methyl rotors that are omnipresent in organic alcohols complicate the analysis, so that not many alcohol clusters have been studied with this technique and its higher-frequency variants. The studied systems include methanol dimer [143], ethanol dimer [91], butan-2-ol dimer [117], and mixed dimers such as propylene oxide with ethanol [144]. The study of alcohol monomers with intramolecular hydrogen-bond-like interactions [102, 110, 129, 145–147] must be mentioned in this context. In a broader sense, this also applies to isolated *n*-alkanols, where a weak C_γ—H$\cdots$O hydrogen bond stabilizes certain conformations [69, 102]. Microwave techniques can also be used to unravel the information contained in the IR spectrum of clusters with high sensitivity [148]. Furthermore, high-resolution UV spectroscopy can provide accurate structural information in suitable systems [149, 150] and thus complement microwave spectroscopy.

B. Infrared Absorption

Infrared spectroscopy is the workhorse in this field, because it can quickly provide dynamical details, discriminate between different cluster sizes and phases [40], and sample a wide spectral range. It often yields valuable feedback for quantum chemical calculations. In contrast to some action spectroscopy techniques, IR absorption spectroscopy is not intrinsically size-selective. All cluster sizes generated in the expansion are observed together, and indirect methods of size assignment are needed.

For the study of alcohol clusters, direct absorption in supersonic jets [151] is particularly powerful. The best compromise between sensitivity, spectral resolution, spectral coverage, reproducibility, and simplicity is probably achieved by the synchronization of pulsed slit jet expansions with FTIR scans [65, 152–154]. One realization is illustrated in Fig. 5. Because this technique uses incoherent light sources, it works best for the large cross sections of hydrogen-bonded O—H stretching fundamentals, but it has also been applied to overtones [89], framework vibrations [65, 155], and even intermolecular modes [93, 156]. Where spectral resolution is more important than spectral coverage, cavity-ring-down laser absorption spectroscopy is a competitive technique [75, 157]. While high spectral resolution can be achieved by both FTIR [158] and laser absorption methods [75, 157], the sensitivity drops significantly with increasing resolution in the FTIR case. Anyway, high spectral resolution is most useful for small monomers and possibly its dimers [158, 159], but not for larger organic clusters.

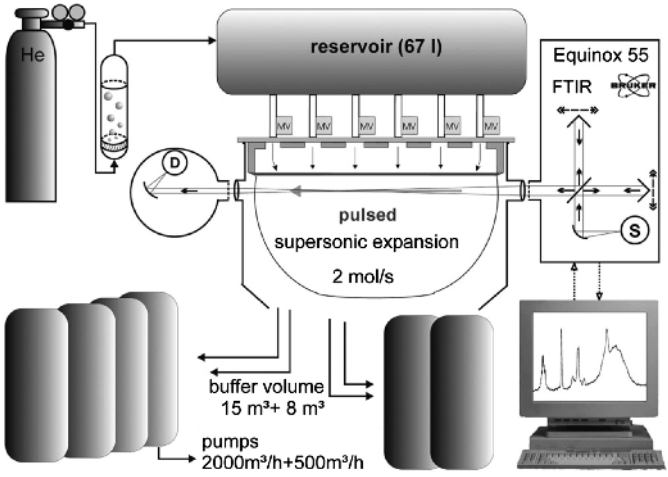

Figure 5. Schematic drawing of a high-throughput pulsed slit jet FTIR setup involving a 600-mm nozzle that is synchronized to the interferometer scans [154].

Infrared absorption spectroscopy is also a powerful tool for matrix isolation studies, which have been carried out extensively for alcohol clusters [34, 88, 103]. Recently, the gap between vacuum and matrix isolation techniques for direct absorption spectroscopy has been closed by the study of nano-matrices—that is, Ar-coated clusters of alcohols [80]. Furthermore, alcohol clusters can be isolated in liquid He nanodroplets, where metastable conformations may be trapped [160].

C. Raman Scattering

Whenever symmetry or quasi-symmetry plays a role, particularly in cyclic alcohol clusters, spontaneous Raman scattering off supersonic jet expansions provides valuable complementary information on the cluster dynamics [16, 77]. Even for nonsymmetric clusters and monomer conformations, it may be used to complement IR spectroscopy, because the Raman rovibrational selection rules often ensure a more narrow band profile [69, 161]. The applicability of spontaneous Raman scattering to jet-generated hydrogen-bonded clusters is a very recent advance [77], whereas it is more established for the characterization of jet expansions in general [162] and complexes of simple molecules [163, 164]. For molecules with a suitable UV chromophore, more sensitive stimulated techniques coupled with ionization or fluorescence [165, 166] can be applied. By using VUV radiation, these techniques may also be useful for aliphatic alcohols [167], although fragmentation issues have to be addressed in detail. The nonlinear CARS technique is more widely applicable [168, 169], but it suffers from the dependence on the square of the molecule density in jet applications.

In condensed phases, the noncoincidence effect between IR and Raman spectra provides insights into the intermolecular coupling [170, 171]. The combination of IR and Raman spectroscopy is also useful in the study of alcohol clusters in the supercritical state [25].

D. Crossed Beam Techniques

Cluster size assignment is often a challenge for direct absorption or light scattering techniques that do not provide reliable mass information. For dimers, a combination of pressure or concentration dependence and spectral survey is usually unambiguous. In favorable cases, this also applies to trimers, tetramers, and maybe pentamers. Beyond that size, some kind of mass information is required. Aliphatic alcohols and their clusters suffer from heavy fragmentation upon ionization. This is also the case for close-to-threshold ionization [172]. If there is no suitable aromatic chromophore for soft ionization, the most important technique involves deflection of the clusters by a crossed rare gas beam [96, 98, 173, 174]. Using this technique, one can bracket the cluster size from above based on the deflection angle and from below based on the largest fragment that is observed.

E. UV–IR Coupling

Once the alcohol or at least the cluster contains a soft ionization or fluorescence chromophore, a wide range of experimental tools opens up. Experimental methods for hydrogen-bonded aromatic clusters have been reviewed before [3, 19, 175]. Fluorescence can sometimes behave erratically with cluster size [176], and short lifetimes may require ultrafast detection techniques [177]. However, the techniques are very powerful and versatile in the study of alcohol clusters. Aromatic homologs of ethanol and propanol have been studied in this way [35, 120, 121, 178, 179]. By comparison to the corresponding nonaromatic systems [69], the O—H$\cdots\pi$ interaction can be unraveled and contrasted to that of O—H$\cdots$F contacts [30]. Attachment of nonfunctional aromatic molecules to nonaromatic alcohols and their clusters can induce characteristic switches in hydrogen bond topology [180], like aromatic side chains [36]. Nevertheless, it is a powerful tool for the size-selected study of alcohol clusters.

In addition, there is a large number of studies involving aromatic alcohols such as phenol [166] or naphthol, which have in part been reviewed before [21]. These include time-resolved studies [21], proton transfer models [181], and intermolecular vibrations via dispersed fluorescence [182]. Such double-resonance and more recently even triple-resonance studies [183] provide important frequency- and time-domain insights into the dynamics of aromatic alcohols, which are not yet possible for aliphatic alcohols.

F. VUV–IR Coupling

In principle, UV–IR coupling becomes more generally applicable at short UV wavelengths, where even aliphatic alcohols and their clusters absorb photons. In a series of recent papers [172, 184, 185], this approach has been explored. For alcohol monomers, the VUV laser photon alone is either not or just barely able to ionize the molecule. Vibrational excitation of the molecule by a preceding IR laser opens either the ionization channel or additional ion fragmentation channels. For hydrogen-bonded alcohol dimers, the employed VUV excitation is typically above the ionization threshold, but the preceding IR laser can induce dissociation of the dimer. This process depletes the ion signal, and the wavenumber dependence of the depletion is interpreted as the vibrational spectrum. As will be discussed later on, severe spectral distortions including spectral broadening, bidirectional signals, and band shifts arise and tend to become worse for larger clusters. Comparison to direct absorption results can shed light onto the underlying mechanisms of the complex high-energy processes. Even the spectroscopy of strongly bound core electrons reveals some sensitivity to the hydrogen bond interaction in alcohols [186], but the sensitivity currently restricts the study to fairly large clusters.

IV. COMPUTATIONAL METHODS

Computational methods that assist the characterization of alcohol cluster dynamics are essential, numerous, and diverse. Here, we can only briefly mention some of them that turn out to be particularly useful for the analysis presented below. Where available, we refer to authoritative reviews on these subjects.

A. Empirical Force Fields

If the investigated systems are large, the accuracy requirements low, and the computational speed demands high, there is no alternative to empirical force fields. The spectroscopic study of small alcohol clusters appears quite orthogonal to these constraints, because the systems are comparatively small, accurate spectra are required, and relatively few dimensions are expected to contribute to the dynamics. Nevertheless, simple pairwise additive empirical force fields [187] can be re-parameterized to become useful for spectroscopic purposes [72]. To avoid individual solutions for every alcohol system, transferable force fields are to be favored [188]. Given a good-quality force field, a range of classical and quantum nuclear dynamics techniques can be applied to extract the spectra (*vide infra*). However, the limits of such approaches are obvious, and they are most useful when interpolating between experimental data. This remains partially true for more sophisticated force fields, even if intra- and intermolecular degrees of freedom are coupled [189]. Therefore, empirical force fields are more frequently applied to the simulation of liquid structure and dynamics and to biomolecule–solvent systems, where they have become invaluable [190].

B. Electronic Structure Calculations

Potential energy hypersurfaces can be generated pointwise by resorting to a plethora of approximations to the solution of the electronic Schrödinger equation. In the early days of hydrogen-bonded cluster investigations, the Hartree–Fock (HF) method was the only useful *ab initio* approach available. Its deficiencies due to the neglect of electron correlation are now well known. In particular, the HF level does not recover the full hydrogen bond energy and vibrational shift. However, fortunate error compensation by basis set superposition errors has often been exploited to provide a reasonable and computationally economic description of some aspects of the hydrogen bond dynamics in alcohol clusters [39, 191]. Considering the current progress in local correlation methods [192], this may not be needed in the future.

An inexpensive access to electron correlation is provided by density functional and hybrid functional techniques. A range of these techniques is implemented in quantum chemistry packages such as Gaussian [193]. They

describe classical hydrogen bond interactions including cooperativity effects reasonably well, in particular in their hybrid variants which include some HF exchange [194]. Therefore, their application to alcohol clusters is very popular [195–197]. Spectroscopic data can be used to explore their limits. For larger alcohols, layered approaches such as ONIOM extend the applicability [38]. However, the fundamental inability of current functionals to describe dispersion forces becomes more and more critical with system size. In this situation, (semi) empirically dispersion-augmented approaches can be of some use [198].

A more rigorous, but also more expensive, approach is Møller–Plesset perturbation theory. Usually, the second-order (MP2) level is employed, but it requires significantly larger basis sets for convergence than Hartree–Fock or density functional approaches. In the prediction of frequency shifts upon hydrogen bond formation, there can be large changes from second to fourth order, with the MP4 results in better agreement with experiment [199].

If affordable, there is a range of very accurate coupled-cluster and symmetry-adapted perturbation theories available which can approach spectroscopic accuracy [57, 200, 201]. However, these are only applicable to the smallest alcohol cluster systems using currently available computational resources. Near-linear scaling algorithms [192] and explicit correlation methods [57] promise to extend the applicability range considerably. Furthermore, benchmark results for small systems can guide both experimentalists and theoreticians in the characterization of larger molecular assemblies.

Spectroscopic applications usually require us to go beyond single-point electronic energy calculations or structure optimizations. Scans of the potential energy hypersurface or at least Taylor expansions around stationary points are needed to extract nuclear dynamics information. If spectral intensity information is required, dipole moment or polarizability hypersurfaces [202] have to be developed as well. If multiple relevant minima exist on the potential energy hypersurface, efficient methods to explore them are needed [203, 204].

C. Internuclear Dynamics

Within the Born–Oppenhimer approximation, the electronic structure is permanently optimized while the dynamics of the nuclei evolves. The latter thus happens on multidimensional potential energy hypersurfaces which are either defined empirically or else derived from solutions of the electronic Schrödinger equation, as outlined above. In the latter case, they may be calculated on the fly or represented on low-dimensional grids or else they have to be approximated by analytical expressions, not unlike the approach employed for empirical force fields. All these strategies are either laborious or computationally demanding and far from routine usage. Except for on-the-fly and to some extent grid methods, they are also highly specific to a given system and cannot be automated easily.

Therefore, a drastic simplification, the so-called double harmonic approximation, is very popular in theoretical cluster spectroscopy. The dependence of the restoring force and of the electric dipole moment on the vibrational displacement from a minimum structure is assumed to be strictly linear, and the resulting linear system of equations is diagonalized to yield harmonic fundamental vibrations (normal modes) and intensities. Analytical derivative techniques render this approximation very efficient from a quantum chemical point of view. Deviations from real spectra are dealt with by scaling approaches, by looking at differences between monomer and cluster fundamentals, and by other error compensation tools. Obviously, interesting dynamical phenomena such as overtone transitions, combination bands, Fermi resonances, vibrational Franck–Condon patterns, torsional modes, tunneling splittings, and other anharmonic effects are not captured by such an approach. Nevertheless, it often provides a useful zero-order picture of the dynamics, unless multiple minima separated by low potential barriers are involved. Often, one does not need the entire set of normal modes but rather only a small subset. In this case, selective algorithms such as mode-tracking can be helpful [122, 205]. For the highly localized O—H stretching vibrations in alcohols, one can even restrict the normal mode analysis to one or a few local modes [80].

Starting from the normal mode approximation, one can introduce anharmonicity in different ways. Anharmonic perturbation theory [206] and local mode models [204] may be useful in some cases, where anharmonic effects are small or mostly diagonal. Vibrational self-consistent-field and configuration-interaction treatments [207, 208] can also be powerful and offer a hierarchy of approximation levels. Even more rigorous multidimensional treatments include variational calculations [209], diffusion quantum Monte Carlo, and time-dependent Hartree approaches [210].

Semiclassical techniques like the instanton approach [211] can be applied to tunneling splittings. Finally, one can exploit the close correspondence between the classical and the quantum treatment of a harmonic oscillator and treat the nuclear dynamics classically. From the classical trajectories, correlation functions can be extracted and transformed into spectra. The particular charm of this method rests in the option to carry out the dynamics on the fly, using Born–Oppenheimer or fictitious Car–Parrinello dynamics [212]. Furthermore, multiple minima on the hypersurface can be treated together as they are accessed by thermal excitation. This makes these methods particularly useful for liquid state or other thermally excited system simulations. Nevertheless, molecular dynamics and Monte Carlo simulations can also provide insights into cold gas-phase cluster formation [213], if a reliable force field is available [189].

Sometimes, it is claimed that the finite temperature in classical simulations accounts for anharmonicity. This may be coincidentally true for nearly

harmonic low-frequency vibrations at environmental temperatures. However, classical molecular dynamics cannot account for the anharmonicity of a high-frequency oscillator like the O—H stretching mode in an alcohol, at least not using reasonable temperatures. To recover the fundamental frequency of such an oscillator, a simulation temperature of more than 5000 K would indeed be needed.

V. SYSTEMS

The alcohols and their clusters will be discussed in order of increasing chemical complexity. With growing complexity, more and more of the issues discussed in Section II come into play and can be addressed by the experimental methods outlined in Section III in combination with computational approaches such as those mentioned in Section IV.

A. Methanol

For organic hydrogen bonds, methanol takes the role that HF has for inorganic hydrogen bonds—it is the simplest conceivable prototype. Its cluster spectroscopy has been reviewed together with that of water clusters [98]. While the monomer vibrational dynamics is in general well-studied [214–217], different values for the fundamental O—H stretching band center are in use [63, 64, 75, 173, 189, 218]. Based on combined Raman and IR evidence, a value of 3684–3686 cm^{-1} appears well-justified [16, 65, 77, 82, 216]. It serves as an important reference for vibrational red shifts in methanol clusters.

The methanol dimer is structurally well-characterized [143]. It features a clear distinction between hydrogen bond donor and acceptor O—H groups. The acceptor band is only slightly shifted to lower wavenumber, relative to the free monomer [75, 77]. It coincides with a monomer transition from the excited methyl rotor tunneling state. The donor band is shifted by 111 cm^{-1} to the red. Harmonic predictions of this red shift are much larger, even at fairly high levels of electronic structure treatment [16]. This may be due to higher-order electron correlation and anharmonic effects [199]. Upon deuteration of the bridging proton, the shift reduces to 80 cm^{-1}, again much less than the best harmonic predictions. Even deuteration of the free O—H group affects the red shift of the hydrogen-bonded O—H noticeably, although the two oscillators are well-decoupled [58]. This confirms the high sensitivity of vibrational frequency shifts to details of the hydrogen bond environment.

The methanol trimer is arguably one of the most interesting clusters. The unexpected structure in its O—H stretching spectrum [65, 75, 77, 173] has only recently found a consistent explanation [16]. It is not related to structural isomers [64, 75, 195, 219, 220] but rather to simultaneous excitation and de-excitation of low-frequency methyl umbrella modes [16, 65], that is, a

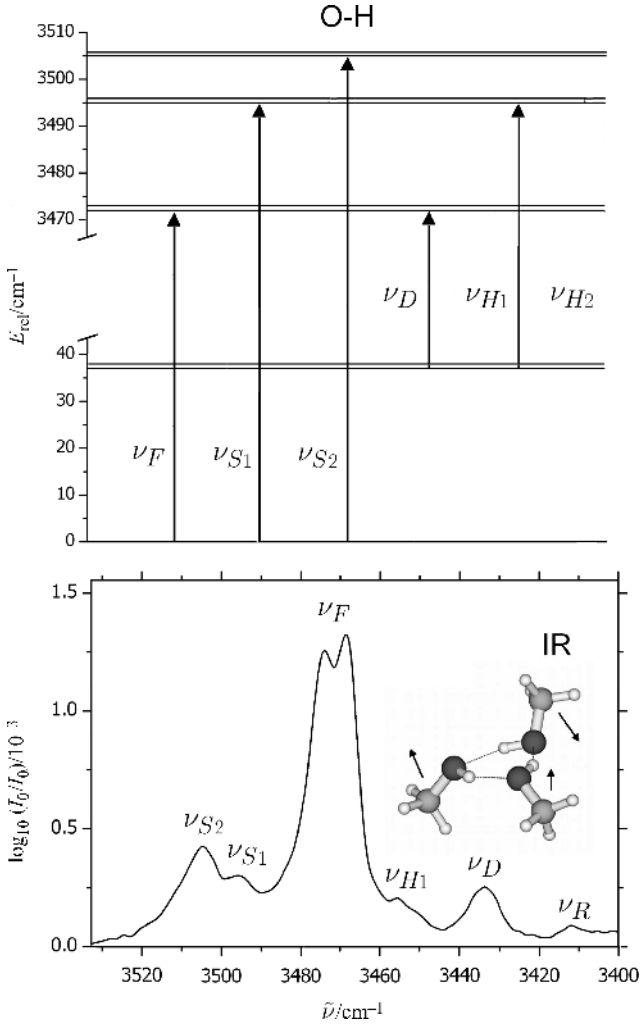

Figure 6. The complex OH stretching spectrum of methanol trimer (**bottom**) can be explained by sum (ν_S), difference (ν_D), and hot bands (ν_H) involving the OH fundamental (ν_F) and two umbrella modes of the methyl groups, which are nearly degenerate in the ground state but soften and split after OH stretching excitation. ν_R is the predominantly Raman active concerted stretching mode [16].

vibrational Franck–Condon effect (see Fig. 6). It is now clear that methanol trimers in free jets only occur in a cyclic, chiral [5] structure, in which two methyl groups point above and one below the hydrogen-bonded plane. This results in two nearly degenerate, strongly IR-active O—H stretching modes and

a very weak but strongly Raman-active in-phase stretching mode [77], similar to the phenol case [166]. Its assignment permits to quantify the average O—H oscillator coupling matrix element around $20\,cm^{-1}$ [16].

In contrast to the unsymmetric trimer, the cyclic tetramer allows for an alternating arrangement of the methyl groups, as one would expect it in a simple lone-pair orbital picture (Fig. 1). The S_4-symmetric structure leads to a symmetric double minimum potential for concerted fourfold proton transfer. This proton transfer has been predicted to be accelerated substantially by symmetric O—H stretching excitation. The predicted tunneling splitting in a reduced dimensionality treatment [106] is on the order of $1\,cm^{-1}$. While this prediction is still uncertain, it presents a challenge for Raman spectroscopic measurements. Currently [16], the upper experimental limit is $7\,cm^{-1}$, in good agreement. Better cooling of the clusters in the Raman jet experiment may help in tightening this experimental bound, but IVR processes in which the energy flows out of the O—H stretching manifold could prevent the detection of a splitting. Energy redistribution within the O—H stretching manifold is characterized by a nearest-neighbor coupling constant of $30\,cm^{-1}$ and a second-nearest neighbor coupling of $10\,cm^{-1}$, that is, it happens on a picosecond time scale [16].

The preparation of single isomers for methanol dimer, trimer, and presumably tetramer [16] in a supersonic jet expansion contrasts the structural diversity that can be prepared and manipulated in cryogenic matrices [34]. It underscores the ability of supersonic jet expansions to funnel all intermolecular isomers down to the global minimum, if there are no major barriers to overcome on the way.

O—H stretching bands of larger methanol clusters start to overlap. Investigations on their dynamics and isomerism [160, 196, 197] typically require size-resolved studies [174]. The recently proposed size-specific VUV-IR technique is not practical for this purpose, because it produces strongly broadened, spectrally shifted and most likely fragmentation-affected bands for methanol trimer and larger clusters [172].

The anharmonicity of the O—H stretching oscillators changes with cluster size. For the monomer, the anharmonicity constant is on the order of $90\,cm^{-1}$. A coarse deuteration analysis [16, 88] suggests that it increases by more than 20% upon trimer and tetramer formation [16]. More accurate overtone analyses are possible in a rare gas matrix [88], but the matrix shift complicates a direct comparison to theory. As an example, the overtone-deduced anharmonicity of methanol monomer in a nitrogen matrix [88] is $85\,cm^{-1}$, whereas in vacuum [16] it is $92\,cm^{-1}$. The deuteration-estimated anharmonicity is $91\,cm^{-1}$ for the monomer and $97\,cm^{-1}$ for the dimer donor in the nitrogen matrix, whereas it is $87\,cm^{-1}$ for the monomer and $89\,cm^{-1}$ for the dimer donor in vacuum. Clearly, only a vacuum overtone measurement would be fully conclusive, but as the matrix study [88]

shows, this is very challenging for methanol dimer and completely out of reach for trimers. However, calculations also support the idea of a moderate increase of anharmonicity upon deuteration in the case of methanol [199].

Instead of embedding methanol clusters in a bulk Ar matrix, one can decorate the preformed clusters with Ar atoms. This nanocoating is observed for Ar as a carrier gas, if the expansion is lean enough in methanol to reach low temperatures. The sign and size of the nanomatrix shifts reflects the cluster–matrix interaction. In the case of the open dimer, a red shift is observed because the Ar atoms can serve as secondary weak hydrogen bond acceptors. The trimer is actually blue-shifted, supporting its closed cycle structure and suggesting that packing effects dominate the matrix interaction [158]. Instead of nanocoating the preformed methanol clusters with Ar, one can also attach more than one methanol unit to preformed Ar clusters using a molecular beam pickup technique [97]. This can result in different cluster structures, although the available results in the C—O stretching region [97] are less straightforward to interpret than O—H stretching data.

Methanol clusters have indeed been studied using several other intramolecular excitations, such as the O—H bending fundamental [88] and the C—O stretching mode [65, 98]. Here, the different cluster sizes are not so well-separated and size resolved methods are helpful. A strong cluster size dependence and mode coupling is observed for intermolecular librational bands, which assisted the assignment of the IR-active libration modes of methanol tetramer in a free jet expansion [93]. They are found to be quite anharmonic. Although these modes correlate with overall rotation and methyl torsion of the monomer, they do not involve significant methyl group motion in the cluster (see also Fig. 3). These individual cluster librational bands are two orders of magnitude more narrow than the overall librational band profile. This shows that the broad librational bands in liquid alcohols are largely due to different hydrogen bond environments, rather than to rapid vibrational energy flow. The librational pattern of the cyclic tetramer spectrum has similarities to that of the extended crystalline solid [40], and the IR intensity of the high-frequency libration band serves as a puckering indicator for the methyl groups (see Fig. 7, band C). The effect of librational and torsional excitation on the O—H overtone dynamics in methanol clusters would be of interest, given the influence detected in the methanol monomer [83]. Furthermore, torsional states offer important doorways for vibrational energy flow in alcohols [142]. At the low-frequency end of methanol cluster dynamics, hindered monomer rotations and translations appear in the IR spectrum [156, 221–223].

When methanol interacts with other molecules, there are some characteristic differences to water [36]. For example, methanol can symmetrically bind two HCl molecules to its lone pairs without significant energy penalty compared to a cooperative ring arrangement [61]. This is not the case for water, because its

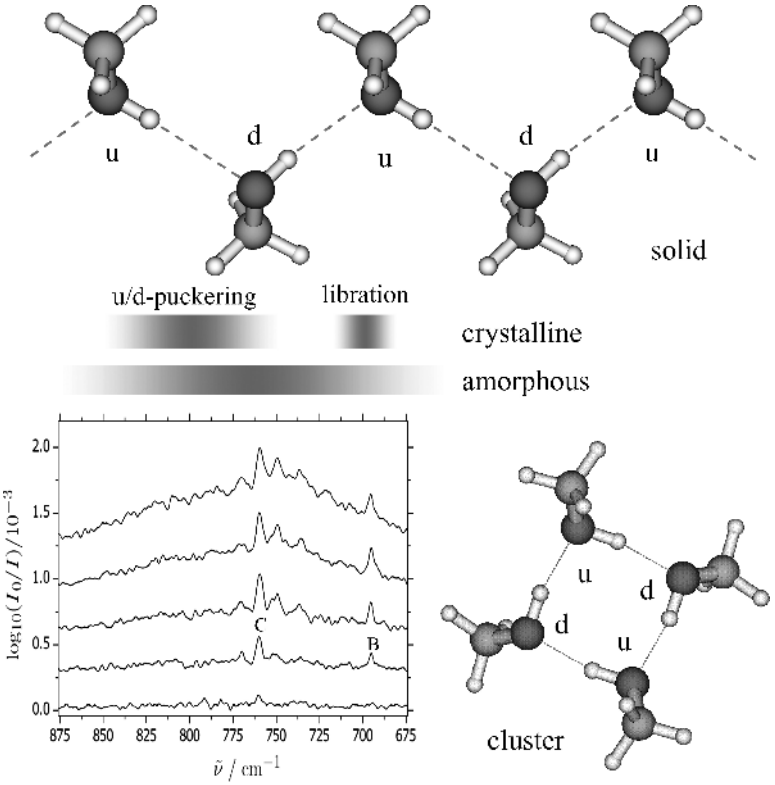

Figure 7. Librational infrared spectra of methanol clusters [93] (bands B and C due to the tetramer, broad profile due to large clusters, cluster size increases from bottom to top) compared to the absorptions in amorphous and crystalline (zig-zag) solid methanol [40]. The large clusters compare well to the amorphous solid, whereas the ring tetramer may be viewed as a small model of the zig-zag chains in the crystal. Note that the high-frequency band C acquires IR intensity through puckering of the methyl groups above (u) and below (d) the hydrogen bond plane.

lone pairs are less electron-rich. Some other complexes of methanol are discussed in the following chapters.

B. Ethanol

Ethanol introduces the issue of conformational isomerism around the C—O bond (Fig. 4, top). The transiently chiral gauche conformations (g+ and g−) are 0.5 kJ/mol higher in energy than the anti or trans form (t) [101]. While the trans form thus dominates at low temperatures in the isolated molecule, crystalline ethanol consists of alternating gauche and trans conformations arranged in infinite hydrogen-bonded chains [224, 225]. To investigate the influence of

aggregation on conformational isomerism, hydrogen-bonded ethanol dimer was studied repeatedly. Out of the nine distinguishable dimer conformers in a simple counting scheme involving acceptor lone pairs [65], about six may be expected to be relatively stable [33]. Earlier theoretical studies were not very conclusive concerning the subtle energy sequence of these isomers. For an accurate theoretical description of dimers, it is essential that the differences in monomer conformation are well-described. Direct absorption measurements in He supersonic jet expansions [65, 157] and Raman jet spectroscopy [77] reveal at least three, more likely four, competing dimer conformers even at low temperatures. They can be converted into a single most stable conformer by adding Ar to the expansion as a relaxation promoter [80]. This global minimum conformation is among the isomers with the strongest red shift. Extensive *ab initio* calculations [80] indicate that it is a homoconfigurational gauche dimer; that is, both ethanol units occur in the less stable gauche conformation and match their helicities. Rewardingly, this conformation also exhibits a strongly red-shifted O—H stretching band in the calculations, in line with the experimental correlation between shift and stability [80]. Hence, the conformational preference of the monomer is reversed in the dimer, although the driving forces behind this isomerization only involve weak hydrogen bonds and dispersion interactions, whereas the classical O—H$\cdots$O hydrogen bond does not discriminate significantly between the conformations. The subtlety of this conformational isomerism is underscored by the fact that matrix embedding of the dimer recovers the trans conformation for both alcohol units [103]. However, spectra recorded immediately after deposition can resemble the jet spectra quite closely under certain conditions [226]. The three most stable dimer conformations according to the correlated *ab initio* calculations [80] are also the ones that are observed in a high-resolution microwave study [91]. The ethanol dimer donor band obtained by the nonresonant ion dip IR technique (i.e., VUV–IR coupling [184]) is broad and unstructured. It falls on the slope of an even broader feature that has the opposite sign; that is, the IR excitation enhances ionization instead of depleting it. The fact that the depletion signal is blue-shifted by more than $30\,\mathrm{cm}^{-1}$ from the narrow and well-structured, true direct absorption or Raman band [65, 77, 80, 157], is probably related to this complex phenomenon.

The O—H stretching spectra of ethanol trimers and larger clusters cannot be conformationally resolved in a slit jet expansion [65, 77, 157]. VUV-IR spectra [184] are even broader, sometimes by an order of magnitude, and band maxima deviate systematically by up to $+50\,\mathrm{cm}^{-1}$ from the direct absorption spectra. We note that ethanol dimers and clusters have also been postulated in dilute aqueous solution and discussed in the context of the density anomaly of water–ethanol mixtures [227]. Recently, we have succeeded in assigning Raman OH stretching band transitions in ethanol·water, ethanol$_2$·water, and ethanol·water$_2$ near 3550, 3410, and $3430\,\mathrm{cm}^{-1}$, respectively [228].

Isolated ethanol clusters have earlier been studied using CO_2 lasers and size-selective action spectroscopy in the C—O stretching range [94]. Attaching or surrounding the ethanol dimer with Ar atoms gives rise to vibrational shifts in both spectral ranges [80, 94]. Mixed dimers of ethanol and methanol have been studied as well [58] and show that methanol prefers to act as a hydrogen bond donor. This is in line with the improved acceptor character of ethanol, caused by the inductive effect of the C_α methyl group. In contrast to ethanol dimer, the trans preference of the acceptor molecule is preserved in this mixed complex. The same is true for phenol–ethanol dimer [229], but in both cases the preference is reduced compared to the monomer. In summary, in a simple but subtle case of conformational control, the preference of ethanol for a stretched trans conformation can be attenuated and inverted by offering it a range of donor alcohol molecules. This control will be lost completely at elevated temperatures, where dynamically assembled ethanol dimers are important for the properties of the supercritical state [24].

C. Linear Alcohols

The dynamical features observed for methanol and ethanol invite an extension to longer alkyl chains, to see whether any new aspects related to the increased conformational freedom come into play. The O—H group is a sensitive probe for at least the nearest-neighbor torsional states [230]. This is already true at room temperature and even more so in supersonic jets [65, 69, 157].

While isolated linear alkanes prefer an all-trans conformation if they are not too long, the presence of a terminal O—H group induces a gauche conformation along the C_α—C_β bond (Gt in propanol; see Fig. 8). The preferred O—H orientation relative to the alkyl backbone remains trans, like in ethanol. This is consistent with the relaxation behavior of *n*-propanol and longer-chain alkanols in supersonic jet expansions [69]. Van der Waals interactions of the oxygen atom with $C_\gamma H$ have been postulated as a reason [69, 231]. However, the all-trans conformation is also quite low in energy [102]. These robust experimental findings encourage accurate quantum chemical studies of the conformational landscape of *n*-alcohols, including higher order electron correlation [69, 232]. Once an accurate description of the potential energy hypersurface is achieved, zero-point energy contributions must be addressed. It remains to be seen whether a consistent picture can be achieved at the harmonic level or whether anharmonic contributions are important in the torsional subspace.

In order to obtain robust conformational assignments from vibrational spectra without rotational resolution, it is important to predict reliable monomer frequency shifts between conformations. Harmonic B3LYP predictions were shown to correlate reasonably well with experiment [69], and simple rules based on repulsive and attractive intra-monomer interactions were developed. However, the predicting power of the B3LYP method for the energy sequence

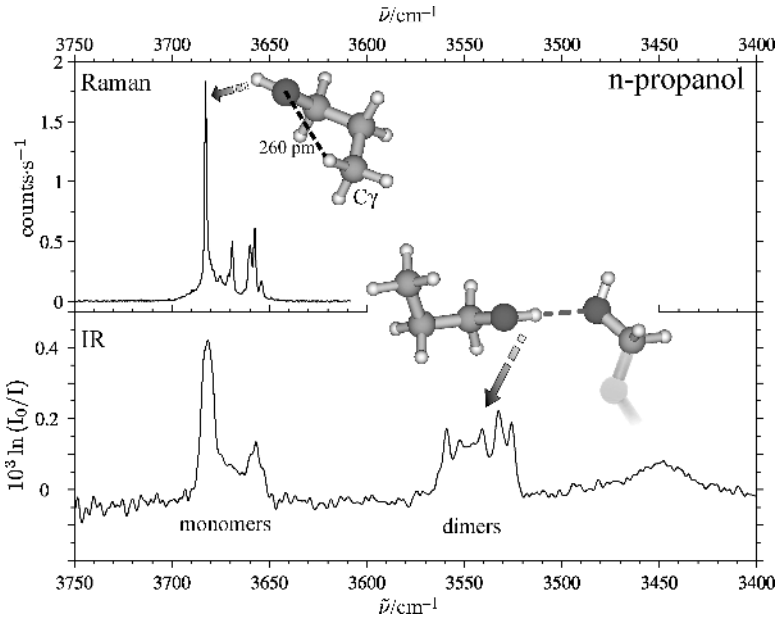

Figure 8. IR and Raman OH stretching spectra of *n*-propanol monomers and dimers reflecting conformational diversity. The Raman spectrum reveals the dominance of the internally hydrogen-bonded Gt monomer most clearly, whereas the IR spectrum indicates more than five different dimer conformations in the red-shifted dimer spectrum [69].

is much inferior [69]. For a spectral separation of the different conformations, Raman spectroscopy proves to be powerful, because the spectra are dominated by narrow Q-branches. Future improvements of the Raman jet setup [77] will also allow for Ar relaxation experiments. Currently, a combination of IR and Raman experiments is most conclusive in the monomer regime.

Beyond ethanol, the number of *n*-alkanol dimer conformations becomes too large to be vibrationally resolved, even in supersonic jets. For *n*-propanol, more than five isomers are discernible in the donor O—H stretching spectrum (see Fig. 8). For longer chains, there is a smaller number of dominant conformations [69]. Ar relaxation shows that the most stable *n*-propanol and *n*-butanol dimers are those with the largest observed red shifts. For longer chains, the situation is more complex. However, the window of observed O—H stretching bands is quite independent of chain length beyond propanol.

A subtle chain-length alternation effect is observed upon coating the alcohol molecules and dimers with Ar. For monomers, the O—H stretching frequency of even-membered chains is perturbed more strongly than that of odd-membered chains. For dimers, the opposite pattern is observed [69]. The modeling of such

subtle embedding effects is challenging [233]. However, it is important, because isomerization studies among the different conformers are most elegantly carried out in cryogenic matrices [103]. Chain length and chain conformation can also influence the energy flow out of the O—H oscillator into the rest of the molecule or molecular cluster [21].

D. Bulky Alcohols

Branching of the alkyl chain attached to the O—H group opens up a variety of perspectives. It increases the bulkiness of the alcohol with consequences for aggregation [234, 235], it allows for the introduction of permanent chirality [117], and it can help to introduce larger energy differences among conformations.

With respect to bulkiness, *t*-butyl alcohol is the simplest monoconformational example. It is therefore investigated intensely and used as a model system for amphiphilic behavior [236]. *t*-Butyl alcohol is thought to form micellar structures or microscopic aggregates in the liquid [13], in aqueous solution [237] and also in the supercritical state [25]. Its crystal structures are diverse and complex [44, 238]. Therefore, the investigation of isolated *t*-butyl alcohol clusters is of some interest. Their O—H stretching infrared spectrum has been characterized [39] and is found to exhibit unusual structure even for larger clusters. The origin of this structured spectrum, which falls in a region of C—H stretch–torsion combinations, remains to be understood in detail. Large cluster formation still appears to be feasible, although the bulky *t*-butyl groups certainly interfere with each other and the tetramer may be viewed as a kind of magic number cluster [213]. This is confirmed by a study of mixed clusters of naphthol and *t*-butyl alcohol [235]. Clusters of even more bulky alcohols such as adamantanols and multiply branched alcohols have been studied [65, 72]. In contrast to earlier evidence around room temperature [37], the low-temperature environment appears to be able to stabilize aggregates beyond the dimer [65]. Crystal structure determination even reveals tetrahedral arrangements of the O—H groups in extremely bulky alcohol tetramers, although the proton positions are disordered [239]. The hydrogen-bond-induced red shift in branched alcohol dimers can be predicted using a fairly simple molecular modeling approach, as long as conformational isomerism does not complicate the picture [72].

With respect to chirality, 2-butanol is the simplest alcoholic model system. Due to a single strong recognition center (the hydrogen-bonded O—H group), the energy differences between a dimer built from homoconfigured (e.g., left-handed) monomers and a dimer between heterocofigured (mixed left- and right-handed) molecules are not very large. Spectral differences in the IR are therefore quite small, whereas conformations of the two diastereomeric dimers can be easily told apart in microwave studies of chirality recognition [117].

E. Unsaturated and Aromatic Alcohols

The simplest unsaturated alcohol with sp^3-carbon O—H is allyl alcohol (propenol). The monomer occurs in two energetically similar conformations in the gas phase [145, 240], which are both stabilized by intramolecular O—H$\cdots\pi$ interactions. The dimer has only been studied in matrix isolation [241]. Spectroscopic evidence for an intermolecular O—H$\cdots\pi$ hydrogen bond was found. A vibrational (IR and Raman) supersonic jet measurement would be able to unravel the different monomer and dimer conformations involved.

Among the unsaturated alcohols involving an O—H group attached to a sp^2 carbon, only the resonance stabilized case of malonaldehyde shall be briefly discussed. It features a strong intramolecular hydrogen bond between the enol O—H and the remaining aldehydic C=O group. The hydrogen atom is bound in a double-minimum potential, and the resulting tunneling splitting [210, 242] has recently been studied as a function of vibrational excitation [155, 243]. Remarkable decreases of the tunneling splitting, equivalent to increases in the tunneling period, have been found for some vibrations [155]. Due to the strong intramolecular hydrogen bond, the clustering tendency of malonaldehyde is small, unless one studies excited conformations [104]. The same applies to tropolone [244].

Aromatic alcohol clusters have been well-studied, also for methodical reasons. The UV chromophore can be exploited for sensitive detection of the IR spectrum [35, 36, 120, 179]. Time-domain experiments become possible [21], which show that the initial energy flow out of the O—H stretching mode occurs primarily via C—H stretching and bending doorway states. Like in the case of carboxylic acid dimers [245], the role of the hydrogen bond is to shift the O—H stretching mode closer to these doorway states and thus to accelerate the initial energy flow.

In terms of binding energy, classical hydrogen bonding may be enhanced by the increased acidity of the phenolic O—H, if the acceptor alcohol is non-phenolic [149, 182]. On the other hand, π interactions compete with classical hydrogen bonds [19, 54] and may even dominate the interaction, such as in the dimer of 1-naphthol [55]. This is not yet the case for phenol dimer, the prototype compound in this class [246, 247].

F. Fluoroalcohols

The hydrogen bonds in aliphatic alcohol clusters can be modified in a systematic, yet subtle, way by replacing hydrogen atoms of the alkyl group by fluorine atoms [248, 249]. This leads to only modest changes in spatial extension, but it introduces polarity into the hydrophobic alkyl chains. Despite their polarity, the fluorine atoms are not considered to be attractive hydrogen bond acceptors [250]. Fluorinated alkanes have quite remarkable properties that can be related to this combination of polarity and weak hydrogen bond propensity. Alcohols with

fluorine atoms at the α-carbon are usually not stable with respect to HF elimination [251, 252]. Therefore, fluorinated ethanols are the simplest stable model systems.

2-Fluoroethanol has been studied in detail. The unsymmetric methyl group substitution increases the number of spectroscopically distinguishable isomers from 2 to 5. However, the intramolecular interaction of the O—H group with the F atom stabilizes one out of these conformations by more than 6 kJ/mol. This is enough to form it almost exclusively under supersonic jet expansion conditions [130]. Even in the room-temperature gas phase, there is no sound evidence for other conformations. There has been a lot of debate on whether this intramolecular O—H···F interaction should be considered a hydrogen bond, given that the arrangement of the three atoms is far from linear. Because analogous intermolecular interactions with more favorable geometry show important features of weak hydrogen bonds [130], we will also discuss the bent intramolecular contact in these terms, being aware of alternative viewpoints [253]. What makes the global minimum structure of fluoroethanol particularly interesting is its chirality, although this chirality is of course not relevant for the conventional spectroscopy of the monomer.

Due to the intramolecular O—H···F contact, hydrogen-bonded 2-fluoroethanol dimers may be expected to be structurally less diverse than ethanol dimers. Indeed, there is no indication for dimers built from metastable monomer conformations in the supersonic jet expansion [130]. However, the fluorine atom of the hydrogen bond donor alcohol can be engaged in a secondary interaction with the O—H group of the acceptor, which would be ''dangling'' in the case of regular ethanol dimers. Depending on whether or not this interaction is established, the dimers are classified as insertion (i) or addition (a) complexes [154]. Insertion means that the acceptor O—H opens and bridges the weak intramolecular O—H···F contact, resulting in a much more favorable and even slightly cooperative O—H···O—H···F arrangement. Addition complexes do not involve such an insertion, but rather conserve the intramolecular contacts of the acceptor and to some extent also of the donor molecule. Obviously, the donor geometry is somewhat distorted by the competition of the acceptor molecule, which is why these complexes have also been called ''associated'' [130].

Considering the chiral nature of the fluoroethanol monomer, one may therefore expect at least four distinguishable dimer conformations. Heterocofigurational (het) or homoconfigurational (hom) pairings may be combined with inserted or associated hydrogen bond topologies. The choice between the two acceptor oxygen lone electron pairs may double this number, but calculations show that one of the lone pairs is usually more attractive than the other, because it allows for a compact (c) rather than open (o) dimer structure, with increased interaction energy.

A supersonic jet spectrum indeed shows evidence for four dimer isomers based on the red-shifted donor O—H stretching vibrations [130]. In the acceptor region, only two bands are observed, the other two most likely overlapping with the monomer band. The fact that they overlap already indicates that they are of the associated type, where the O—H group remains largely unaffected. Stronger evidence comes from an Ar relaxation study. Already traces of the more efficient relaxation promoter are enough to deplete the two least red-shifted donor bands, whereas the two acceptor bands persist. Therefore, a picture analogous to that in ethanol dimer emerges. The most stable dimers exhibit the strongest red shifts and are thus of the inserted type. Calculations suggest that the energy difference is quite subtle, making this a suitable reference system for quantum chemical calculations of weak secondary interactions. Chirality recognition is only weak, but the experimental evidence indicates that the heteroconfigurational dimer may be slightly more stable, opposite to the case of ethanol.

We note that 2,2-difluoroethanol behaves quite similar to fluoroethanol. Again, there is only one dominant monomer conformation and up to four dimer isomers are observed. However, in this case the relaxation behavior is completely opposite. The least red-shifted isomers are now most stable and correlate well with associated complexes. This illustrates the subtle interplay between weak O—H$\cdots$F hydrogen bonds and similarly weak C—H$\cdots$F interactions, which can also form, even in associated complexes.

Fluorinated alcohols are not only interesting as model systems for weak hydrogen bonds with implications in the life sciences [254] and as chemical sensor materials [255], but also provide excellent reaction media [256, 257] and peptide solvents [258–260] with conformation-modulating properties. In both cases, molecular aggregates are thought to play an important role. One of the most widely used fluorinated alcohols is 2,2,2-trifluoroethanol, which will be in the focus of the following section.

G. Trifluoroalcohols

Trifluoromethanol is only metastable with respect to decomposition into $F_2C{=}O$ and HF [261]. The simplest stable alcohol with a CF_3 group is 2,2,2-trifluoroethanol. Like ethanol, it can occur in a gauche and a trans conformation, but the transiently chiral gauche conformation [146, 262] is strongly favored over the trans form due to intramolecular interactions [263]. It is actually questionable whether the trans form represents a stable local minimum in the isolated molecule [30], whereas it has been found to be abundant in the liquid [264]. It is therefore of interest to investigate for which cluster size the trans conformation starts to become important. The interconversion between the two gauche forms of trifluoroethanol is an order of magnitude slower than in ethanol [146], a consequence of the stabilization of the gauche forms due to the

intramolecular contact. On the other hand, the anharmonicity of the O—H oscillator in gauche trifluoroethanol [30] ($\omega_e x_e = 85\,\mathrm{cm}^{-1}$) is comparable to that of ethanol monomer [81, 265] ($\omega_e x_e = 88\,\mathrm{cm}^{-1}$), based on fundamental and overtone data [89] (see Fig. 2).

In analogy to fluoroethanol, which is also locked in a chiral gauche conformation, one would expect to observe up to four trifluoroethanol dimer conformations, differing in their hydrogen bond topology (inserted versus associated) and in their relative monomer chirality or helicity (hom versus het). Calculations suggest that two of these may not be present in large abundance, because they are higher in energy by a few kJ/mol, whereas the other two are predicted to be energetically nearly degenerate (see Fig. 9). However, the experimental spectra [30, 76] (see Fig. 2) strongly support a single dimer conformation, even under the mildest expansion conditions, where relaxation over barriers of more than a few kJ/mol should be inhibited. The spectral details are consistent with a homoconfigurational inserted dimer; that is, both monomer units have the same helicity sense and the acceptor O—H inserts into the intramolecular contact of the donor, forming a weak O—H$\cdots$F hydrogen bond. The energetically almost equivalent heteroconfigurational isomer without insertion is not observed. O—H torsional tunneling between the enantiomeric forms of the dimer should be efficiently quenched. Interconversion between the two nearly isoenergetic, but topologically different, isomers involves a barrier of close to 10 kJ/mol (see Fig. 9). Therefore, it is not easy to explain the complete

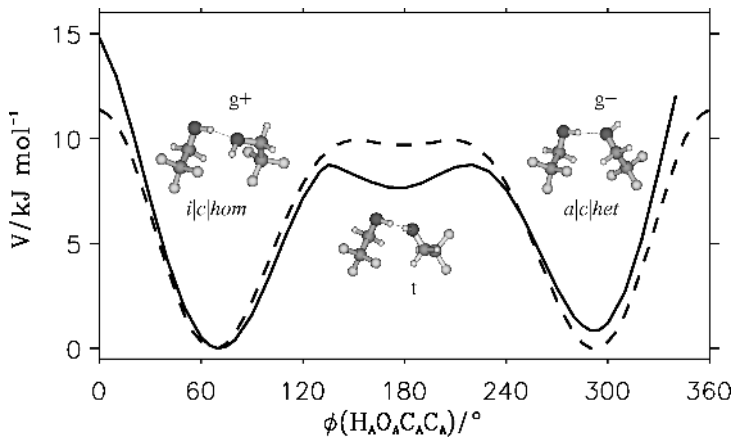

Figure 9. The torsional potential of trifluoroethanol (*dashed line*, g+/t/g−, in analogy to the ethanol case shown in Fig. 4) is only distorted slightly if it acts as a hydrogen bond acceptor toward a g+ trifluoroethanol unit [30] (*full line*). Nevertheless, only the compact inserted homochiral dimer (**left**, *i*|*c*|*hom*) is observed in the jet experiment, not the compact associated heterochiral dimer (**right**, *a*|*c*|*het*).

absence of the heteroconfigurational isomer in a helium supersonic jet expansion, if it is nearly isoenergetic to the homoconfigurational dimer. It remains to be seen which mechanism is responsible for this extreme form of chirality synchronization [30, 76]. In ethanol [80], the addition of an efficient collision partner (Ar) was required to induce relaxation over barriers on the order of only 3 kJ/mol [33] into the global homoconfigurational minimum structure. A transient mechanism proposed recently for isotope-labeled benzene dimer isomerization [266] does not apply to the high-barrier situation in trifluoroethanol dimer. Molecular dynamics simulations of the collisional cooling process using model potentials [72, 267] or preferably quantum chemical calculations [30, 268] might shed some light onto this interesting dynamical process, as would microwave structural information [91].

Trifluoroethanol dimer is also an ideal model system to investigate the influence of hydrogen bonding on O—H stretching anharmonicity. While an isotope study indicated only moderate changes in anharmonicity [30], the recent direct observation of overtone transitions [89] shows that classical hydrogen bonding to oxygen increases the monomer anharmonicity by about 15%, whereas hydrogen bonding to fluorine indeed preserves it (see Fig. 2). In this study, it was possible to quantify the intensity drop from the fundamental O—H transition to the overtone for the first time in an alcohol dimer. The O—H group bound to fluorine experiences a drop by a factor of 30 in band strength, still comparable to that of the monomer [13]. However, the O—H stretching mode facing the oxygen atom of the neighboring molecule drops by a factor of 400, when going from the fundamental to the overtone [89]. This explains on a quantitative level why it is so difficult to observe hydrogen-bonded overtone vibrations and thus to extract reliable anharmonicities.

Moving to larger clusters, there is some indirect spectroscopic evidence that monomer trans conformations start to play a role [30] in the few trimer structures which are stable in a supersonic jet expansion. In contrast to methanol trimer [65, 77], the two most strongly IR-active O—H stretching modes are split significantly and the in-phase stretching mode gathers substantial IR intensity. The analysis of the coupling pattern [30] confirms the lack of quasi-symmetry and suggests the involvement of different monomer conformations in the trimer. Analysis of the deuterated trimer indicates an increased anharmonicity of the O—H stretching mode and pronounced cooperativity effects. According to model simulations and liquid state studies [264], the trans fraction increases with cluster size, until it is comparable to the gauche fraction. A detailed characterization of the solution dynamics of trifluoroethanol is essential for a deeper understanding of its protein solvation and conformational modulation aspects [260].

While the O—H stretching mode is a sensitive indicator of weak hydrogen bonds to fluorine and the hydrogen bond topology, there are other dynamical

consequences of such interactions. C—H stretching modes that are in direct contact with F atoms shift characteristically [30]. This is also evident in a comparison of gas- and liquid-state spectra of such alcohols. Similar effects of fluorination have been studied in clusters between alcohols and aromatic compounds [112, 175, 219].

Beyond trifluoroethanol, new aspects come into play. By fluorinating a methyl group in 2-propanol, permanent chirality can be introduced into the molecule [269, 270]. Substitution of both methyl groups by CF_3 simplifies the isomer pattern, because the resulting hexafluoroisopropanol favors the nonchiral trans conformation [269]. Currently, we are investigating the influence of aliphatic chain length on the interaction of the CF_3 group with the alcohol function in linear trifluoroalkanols and the resulting competition between intramolecular folding and intermolecular aggregation.

H. Chlorinated Alcohols

Chlorinated methanols are only metastable [271], like their fluorinated counterparts. Chlorinated ethanols are stable. Like fluorinated alcohols, they are popular as solvents for peptides [272] because of their characteristic hydrogen bonding properties. Trichloroethanol shows a weaker tendency to dimerize than trifluoroethanol, whereas further aggregation is more favorable, according to solution studies [141]. Matrix isolation studies are also available [262, 273]. We are currently investigating the jet spectra of 2,2,2-trichloroethanol and its clusters. In contrast to trifluoroethanol, more than one dimer conformation is found, thus underscoring the singularity of the previously described chirality synchronization phenomenon. Some chloropropanols are permanently chiral variants of 2-chloroethanol and therefore show a preference between the two gauche conformations that are stabilized by an intramolecular hydrogen bond. This intramolecular case of chirality induction has been investigated by microwave spectroscopy [129].

I. Ester Alcohols

Like O—H groups, carbonyl groups are of major importance in biomolecules and their function. Therefore, an interesting class of model compounds is represented by hydroxyesters. Glycolates are the simplest representatives. They form clusters in which O—H$\cdots$O—H hydrogen bonds compete with O—H$\cdots$C=O hydrogen bonds. The latter are intrinsically stronger, but the former offer cooperative enhancement, if more than two O—H groups are involved [274]. When a methyl group is added to the O—H-carrying carbon, a chiral center is created in the immediate neighborhood of the O—H group. This leads to fascinating chirality recognition phenomena in lactates, in which the relative handedness of neighboring lactate units decides about the preferred hydrogen bond topology in a tetrameric cluster [122, 125, 275]. This tetramer features one of the most

complex gas-phase chirality discrimination phenomena that have been structurally characterized to date. An even more complex alcoholic system involving chirality discrimination is the protonated serine octamer, which has been largely studied via mass spectrometry [15, 123, 124]. Hydroxyesters have also been combined with simple aliphatic and aromatic alcohols [126, 154] to investigate chirality recognition phenomena, the question of kinetic versus thermodynamic control, and more generally the preference for insertion or addition complexes.

J. Polyols and Sugars

While the hydrogen-bond-driven aggregation of isolated O—H groups is now understood fairly well, nature usually employs sugars [59] for molecular recognition tasks [17]. From a hydrogen bond perspective, sugars can be mimicked most easily by polyols, molecules with multiple O—H groups attached to an aliphatic backbone.

The strength of intramolecular hydrogen bonds in diols can be tuned via the distance of the two O—H groups at the carbon backbone [276]. Glycol as the simplest representative of 1,2-diols has been studied extensively in a range of temperatures [277], including supersonic jet and other rotational spectroscopy techniques [278]. By replacing two C—H bonds by C—CH_3 groups, chirality is introduced and diastereoisomerism as an intramolecular variant of chirality recognition occurs [110]. 1,2-Diols can be used to observe hydrogen-bonded O—H overtones [276, 277], because the intramolecular constraints prevent an optimum hydrogen bond geometry. This may reduce the cancellation effect between electrical and mechanical anharmonicity. The liquid state of glycol has been investigated by a range of methods including the development of model potentials [279]. Therefore, isolated cluster studies of this elementary bifunctional prototype would be desirable. The prototype for molecules involving three alcohol groups is glycerol. Its hydrogen bond topology [280, 281] is strongly temperature-dependent, and conformer relaxation in the jet expansion [282] appears to be efficient.

In order to model sugars more closely, further functionalities have to be included. Glycidol may be considered as a simplified model that includes an O-heterocycle. Its dimer has been studied successfully with respect to chirality recognition phenomena [111]. More realistic models for open sugars involve keto or aldehyde groups. Glycolaldehyde may thus be viewed as the simplest realistic sugar model, a diose. Its transition from the internally hydrogen-bonded gas-phase structure to the intermolecular C=O/O—H hydrogen bond network in aggregates has been studied by vibrational spectroscopy [283]. In the thermodynamically stable solid, the carbonyl groups are absent due to chemical dimerization. Higher homologs such as dihydroxyacetone also show an interesting interplay between chemically and hydrogen-bond-directed aggregation [284]. Larger sugars [17, 207, 285], their adducts [286], and their

aggregates up to amorphous sugar nanoparticles [284, 287, 288] as well as sugars in solution [29] represent systems of increasing complexity in which the essential binding motifs of the smaller models can be identified. While experimental data on sugars may not always be conclusive for the properties of isolated hydrogen bonds [32], the opposite is certainly true. By studying clustering in alcohols of increasing complexity and poly-functionality, one will ultimately arrive at an even more detailed understanding of the dynamics and aggregation of naturally occurring mono- [59] and oligo-saccharides [17], which are thought to play a key role in cellular recognition.

VI. CONCLUSIONS

This review has discussed alcohol clusters from methanol [98] to sugars [17]. It has tried to show that a reductionist gas-phase spectroscopy approach to the complexity of organic and biomolecular matter can be fruitful. By studying the most elementary model systems, one can extract the structural, energetic, and dynamic essentials from the enormous hyperspace spanned by the myriads of degrees of freedom involved in biological systems, hydrogen-bonded liquids, and polymers. These essentials include conformational dynamics, molecular recognition, cooperativity, and solvation, among other things. More often than not, one finds that weak hydrogen bonds are decisive for the detailed conformation of alcohols and their complexes.

Infrared, Raman, microwave, and double resonance techniques turn out to offer nicely complementary tools, which usually can and have to be complemented by quantum chemical calculations. In both experiment and theory, progress over the last 10 years has been enormous. The relationship between theory and experiment is symbiotic, as the elementary systems represent benchmarks for rigorous quantum treatments of clear-cut observables. Even the simplest cases such as methanol dimer still present challenges, which can only be met by high-level electron correlation and nuclear motion approaches in many dimensions. On the experimental side, infrared spectroscopy is most powerful for the O—H stretching dynamics, whereas double resonance techniques offer selectivity and Raman scattering profits from other selection rules. A few challenges for accurate theoretical treatments in this field are listed in Table I.

Although most of the reported gas-phase experiments do not investigate the temporal evolution of alcohol clusters explicitly, the frequency-domain spectral information can nevertheless be translated into the time domain, making use of some elementary and robust relationships between spectral and dynamical features [289]. According to this, the 10-fs period of the hydrogen-bonded O—H oscillator is modulated and damped by a series of other phenomena. Energy flow into doorway states is certainly slower than for aliphatic C—H bonds [290]; but on a time scale of a few picoseconds, energy will nevertheless have

TABLE I
Some Challenging Benchmarks for Theoretical Studies of Alcohols and Their Clusters[a]

Quantity	Value	Computational Challenge
ν_{OH} methanol dimer red shift [16]	$111\,cm^{-1}$	Anharmonic value
$(CH_3OH)_4$ proton tunneling period [16] in ν_{OH}^{sym}	$> 5\,ps$	Multidimensional excited state
$(CH_3OH)_4$ anharmonic librational modes [93]	$695/760\,cm^{-1}$	Anharmonic prediction
Homochiral gauche ethanol dimer red shift [80]	$128\,cm^{-1}$	Global minimum property
n-Alkanol Ar coating shift alternation [69]	Odd/even	Van der Waals forces
Torsional malonaldehyde tunneling deceleration [155]	$6\times$	Full-dimensional treatment
Trifluoroethanol chirality synchronization [30]	$> 95\%$	Isomerization profile/dynamics
Size-independent IP for $Na(CH_3OH)_n$ clusters [48]	$n > 5$	Theoretical explanation

[a]See text for details.

dissipated into other, non-O—H stretching degrees of freedom. On its way, it may oscillate or dissipate among coupled O—H oscillators; in special cases, it may even be carried over to neighboring molecules by concerted hydrogen transfer—that is, by explicit mass flow. Where available [21], time-resolved studies confirm this basic picture. Deuteration tends to stretch all these time scales [16, 21, 79]. The role of librations—that is, vibrations of the hydrogens orthogonal to the bridging direction—remains to be explored in detail. Supersonic jet data confirm that much of the breadth of liquid-state O—H stretching bands has an inhomogeneous origin. It arises from different hydrogen bond environments of the local oscillators, although some intrinsic, homogeneous width of the bands persists. In summary, alcohols are interesting by themselves, but are also useful test cases for a range of concepts in vibrational dynamics.

The connection between alcohol clusters and the liquid is probably not as simple as quantum cluster equilibrium studies may imply [45], but their success suggests that the remaining deficiencies are of a subtle topological nature and do not affect energies too much [44]. Energetically, the decisive topological feature is a strong tendency for one-dimensional aggregation, either as chains or as rings.

The future challenges in this field are manifold. The experimental methods must be extended to larger molecular systems and to van der Waals modes [156]. Selectivity in terms of cluster size and conformation will become crucial. Extension to the O—H overtone region and to intermolecular modes will be essential for the characterization of anharmonicity effects. The systematic introduction of further functional groups aside the hydroxy group and the stepwise introduction of solvent effects will increase the biological relevance of the investigated systems. Supramolecular dynamics can be studied and understood in the gas phase.

A systematic study of chlorinated and fluorinated ethanol dimers has recently been published [291].

Acknowledgments

I owe many thanks to my current and former co-workers, whose essential contributions on the dynamics of alcohol clusters are reflected in the cited references. Like me, quite a few of them coincidentally consume more alcohol in research than at social occasions. I also wish to thank my colleagues and collaborators in this field, listed in the cited references. I apologize for any important omissions, which seem unavoidable in such a wide field. Furthermore, I wish to thank the Göttingen mechanical workshops for their competent technical realization of the high-throughput supersonic jet experiments. I acknowledge the generous and flexible financial support by the Fonds der Chemischen Industrie, by the collaborative research centers SFB 357 and SFB 602, by the DFG research training group 782 (www.pcgg.de), and more recently also by the Raman DFG grant Su 121/2.

References

1. L. P. Kuhn, The hydrogen bond. I. Intra- and intermolecular hydrogen bonds in alcohols. *J. Am. Chem. Soc.* **74**, 2492–2499 (1952).
2. D. S. Dwyer and R. J. Bradley, Chemical properties of alcohols and their protein binding sites. *Cell. Mol. Life Sci.* **57**, 265–275 (2000).
3. B. Brutschy and P. Hobza, Van der Waals molecules III: Introduction. *Chem. Rev.* **100**, 3861–3862 (2000).
4. F. N. Keutsch and R. J. Saykally, Water clusters: Untangling the mysteries of the liquid, one molecule at a time. *Proc. Natl. Acad. Sci. USA* **98**, 10533–10540 (2001).
5. W. O. George, B. F. Jones, and R. Lewis, Water and its homologues: A comparison of hydrogen-bonding phenomena. *Philos. Trans. R. Soc. A* **359**, 1611–1629 (2001).
6. J.-M. Lehn, *Supramolecular Chemistry*, Wiley-VCH, New York, 1995.
7. C. Pratt Brock and L. L. Duncan. Anomalous space-group frequencies for monoalcohols C_nH_mOH. *Chem. Mater.* **6**, 1307–1312 (1994).
8. K. J. Gaffney, I. R. Piletic, and M. D. Fayer, Hydrogen bond breaking and reformation in alcohol oligomers following vibrational relaxation of a non-hydrogen-bond donating hydroxyl stretch. *J. Phys. Chem. A* **106**, 9428–9435 (2002).
9. K. J. Gaffney, Paul H. Davis, I. R. Piletic, N. E. Levinger, and M. D. Fayer, Hydrogen bond dissociation and reformation in methanol oligomers following hydroxyl stretch relaxation. *J. Phys. Chem. A* **106**, 12012–12023 (2002).
10. E. T. J. Nibbering and T. Elsaesser, Ultrafast vibrational dynamics of hydrogen bonds in the condensed phase. *Chem. Rev.* **104**, 1887–1914 (2004).
11. J. B. Asbury, T. Steinel, and M. D. Fayer, Hydrogen bond networks: Structure and evolution after hydrogen bond breaking. *J. Phys. Chem. B* **108**, 6544–6554 (2004).
12. K. R. Wilson, R. D. Schaller, D. T. Co, R. J. Saykally, B. S. Rude, T. Catalano, and J. D. Bozek, Surface relaxation in liquid water and methanol studied by x-ray absorption spectroscopy. *J. Chem. Phys.* **117**, 7738–7744 (2002).
13. A. Perera, F. Sokolić, and L. Zoranić, Microstructure of neat alcohols. *Phys. Rev. E* **75**, 060502(R) (2007).
14. W. Weltner, Jr., and K. S. Pitzer, Methyl alcohol: The entropy, heat capacity and polymerization equilibria in the vapor, and potential barrier to internal rotation. *J. Am. Chem. Soc.* **73**, 2606–2610 (1951).

15. B. Baytekin, H. T. Baytekin, and C. A. Schalley, Mass spectrometric studies of non-covalent compounds: Why supramolecular chemistry in the gas phase. *Org. Biomol. Chem.* **4**, 2825–2841 (2006).
16. R. Wugt Larsen, P. Zielke, and M. A. Suhm. Hydrogen-bonded OH stretching modes of methanol clusters: A combined IR and Raman isotopomer study. *J. Chem. Phys.* **126**, 194307 (2007).
17. J. P. Simons, R. A. Jockusch, P. Çarçabal, I. Hünig, R. T. Kroemer, N. A. Macleod, and L. C. Snoek, Sugars in the gas phase. Spectroscopy, conformation, hydration, co-operativity and selectivity. *Int. Rev. Phys. Chem.* **24**, 489–531 (2005).
18. The Thomson Corporation, *ISI Web of Science*, 2007.
19. T. S. Zwier, The spectroscopy of solvation in hydrogen-bonded aromatic clusters. *Annu. Rev. Phys. Chem.* **47**, 205–241 (1996).
20. M. Mons, I. Dimicoli, and F. Piuzzi, Gas phase hydrogen-bonded complexes of aromatic molecules: Photoionization and energetics. *Int. Rev. Phys. Chem.* **21**, 101–135 (2002).
21. Y. Yamada, Y. Katsumoto, and T. Ebata, Picosecond IR-UV pump-probe spectroscopic study on the vibrational energy flow in isolated molecules and clusters. *Phys. Chem. Chem. Phys.* **10**, 1170–1185 (2007).
22. J. S. Lomas, Self- and hetero-association of sterically hindered tertiary alcohols. *J. Phys. Org. Chem.* **18**, 1001–1012 (2005).
23. T. Steiner, The hydrogen bond in the solid state. *Angew. Chem. Int. Ed.* **41**, 48–76 (2002).
24. S. J. Barlow, G. V. Bondarenko, Y. E. Gorbaty, T. Yamaguchi, and M. Poliakoff, An IR study of hydrogen bonding in liquid and supercritical alcohols. *J. Phys. Chem. A* **106**, 10452–10460 (2002).
25. J.-M. Andanson, J.-C. Soetens, T. Tassaing, and M. Besnard, Hydrogen bonding in supercritical *tert*-butanol assessed by vibrational spectroscopies and molecular-dynamics simulations. *J. Chem. Phys.* **122**, 174512 (2005).
26. T. Yamaguchi, New horizons in hydrogen bonded clusters in solution. *Pure Appl. Chem.* **71**, 1741–1751 (1999).
27. A. J. Barnes, H. E. Hallam, and D. Jones, Vapour phase infrared studies of alcohols: I. Intramolecular interactions and self-association. *Proc. R. Soc. London A* **335**, 97–111 (1973).
28. D. R. Miller, Free jet sources, in *Atomic and Molecular Beam Methods*, G. Scoles, ed., University Press, Oxford, 1988, Chapter 2, pp. 14–53.
29. N. A. Macleod, C. Johannessen, L. Hecht, L. D. Barron, and J. P. Simons, From the gas phase to aqueous solution: Vibrational spectroscopy, Raman optical activity and conformational structure of carbohydrates. *Int. J. Mass Spectrom.* **253**, 193–200 (2006).
30. T. Scharge, C. Cézard, P. Zielke, A. Schütz, C. Emmeluth, and M. A. Suhm, A peptide co-solvent under scrutiny: Self-aggregation of 2,2,2-trifluoroethanol. *Phys. Chem. Chem. Phys.* **9**, 4472–4490 (2007).
31. I. Olovsson, The role of the lone pairs in hydrogen bonding. *Z. Phys. Chem.* **220**, 963–978 (2006).
32. J. Kroon, J. A. Kanters, J. G. C. M. van Duijneveldt–van de Rijdt, F. B. van Duijneveldt, and J. A. Vliegenthart, O–H$\cdots$O hydrogen bonds in molecular crystals. A statistical and quantum-mechanical analysis. *J. Mol. Struct.* **24**, 109–129 (1975).
33. V. Dyczmons, Dimers of ethanol. *J. Phys. Chem. A* **108**, 2080–2086 (2004).

34. S. Coussan, A. Loutellier, J. P. Perchard, S. Racine, A. Peremans, A. Tadjeddine, and W. Q. Zheng, Infrared laser induced isomerization of methanol polymers trapped in nitrogen matrix. I. Trimers. *J. Chem. Phys.* **107**, 6526–6540 (1997).

35. K. Le Barbu-Debus, N. Seurre, F. Lahmani, and A. Zehnacker-Rentien, Formation of hydrogen-bonded bridges in jet-cooled complexes of a chiral chromophore as studied by IR/UV double resonance spectroscopy. ±2-Naphthyl-1-ethanol/$(\text{methanol})_{n=1,2}$ complexes. *Phys. Chem. Chem. Phys.* **4**, 4866–4876 (2002).

36. N. Seurre, J. Sepioł, F. Lahmani, A. Zehnacker-Rentien, and K. Le Barbu-Debus, Vibrational study of the S_0 and S_1 states of 2-naphthyl-1-ethanol/ $(\text{water})_2$ and 2-naphthyl-1-ethanol/ $(\text{methanol})_2$ complexes by IR/UV double resonance spectroscopy. *Phys. Chem. Chem. Phys.* **6**, 4658–4664 (2004).

37. F. A. Smith and E. C. Creitz, Infrared studies of association in eleven alcohols. *J. Res. Natl. Bur. Standards* **46**(2), 145–164 (1951).

38. M. M. Pires and V. F. DeTuri, Structural, energetic, and infrared spectra insights into methanol clusters $(CH_3OH)_n$, for $n = 2$–12, 16, 20. ONIOM as an efficient method of modeling large methanol clusters. *J. Chem. Theory Comput.* **3**, 1073–1082 (2007).

39. D. Zimmermann, T. Häber, H. Schaal, and M. A. Suhm, Hydrogen-bonded rings, chains and lassos: The case of *tert*-butyl alcohol clusters. *Mol. Phys.* **99**, 413–426 (2001).

40. M. Falk and E. Whalley, Infrared spectra of methanol and deuterated methanols in gas, liquid, and solid phases. *J. Chem. Phys.* **34**, 1554 (1961).

41. W. Saenger and K. Lindner, OH clusters with homodromic circular arrangement of hydrogen bonds. *Angew. Chem., Int. Ed.* **19**, 398–399 (1980).

42. R. Taylor and C. F. Macrae, Rules governing the crystal packing of mono- and dialcohols. *Acta Cryst. B (Struct. Sci.)* **57**, 815–827 (2001).

43. A. García Fraile, D. G. Morris, A. García Martínez, S. de la Moya Cerero, K. W. Muir, K. S. Ryder, and E. Teso Vilar. Self-recognition and hydrogen bonding by polycyclic bridgehead monoalcohols. *Org. Biomol. Chem.* **1**, 700–704 (2003).

44. P. A. McGregor, D. R. Allan, S. Parsons, and S. J. Clark, Hexamer formation in tertiary butyl alcohol (2-methyl-2-propanol, $C_4H_{10}O$). *Acta Cryst. B (Struct. Sci.)* **62**, 599–605 (2006).

45. R. Ludwig, The structure of liquid methanol. *ChemPhysChem* **6**, 1369–1375 (2005).

46. P. Raveendran, D. Zimmermann, T. Häber, and M. A. Suhm, Exploring a hydrogen-bond terminus: Spectroscopy of eucalyptol–alcohol clusters. *Phys. Chem. Chem. Phys.* **2**, 3555–3563 (2000).

47. A. Fujii, S. Enomoto, M. Miyazaki, and N. Mikami, Morphology of protonated methanol clusters: An infrared spectroscopic study of hydrogen bond networks of $H^+(CH_3OH)_n$ ($n = 4$–15). *J. Phys. Chem. A* **109**, 138–141 (2005).

48. I. Dauster, M. A. Suhm, U. Buck, and T. Zeuch, Experimental and theoretical study of the microsolvation of sodium atoms in methanol clusters: Differences and similarities to sodium-water and sodium-ammonia. *Phys. Chem. Chem. Phys.* **10**, 83–95 (2008).

49. A. Latini, D. Toja, A. Giardini-Guidoni, S. Piccirillo, and M. Speranza, Energetics of molecular complexes in a supersonic beam: A novel spectroscopic tool for enantiomeric discrimination. *Angew. Chem. Int. Ed.* **38**, 815–817 (1999).

50. M. Mons, F. Piuzzi, I. Dimicoli, A. Zehnacker, and F. Lahmani, Binding energy of hydrogen-bonded complexes of the chiral molecule 1-phenylethanol, as studied by 2C-R2PI: Comparison between diastereoisomeric complexes with butan-2-ol and the singly hydrated complex. *Phys. Chem. Chem. Phys.* **2**, 5065–5070 (2000).

51. C. Wickleder, D. Henseler, and S. Leutwyler, Accurate dissociation energies of O–H···O hydrogen-bonded 1-naphthol·solvent complexes. *J. Chem. Phys.* **116**, 1850–1857 (2002).
52. A. Bizzarri, S. Stolte, J. Reuss, J. G. C. M. van Duijneveldt–van de Rijdt, and F. B. van Duijneveldt, Infrared excitation and dissociation of methanol dimers and trimers. *Chem. Phys.* **143**, 423–435 (1990).
53. L. Belau, K. R. Wilson, S. R. Leone, and M. Ahmed, Vacuum ultraviolet (VUV) photoionization of small water clusters: Correction. *J. Phys. Chem. A* **111**, 10885–10886 (2007).
54. K. Le Barbu, V. Brenner, Ph. Millié, F. Lahmani, and A. Zehnacker-Rentien, An experimental and theoretical study of jet-cooled complexes of chiral molecules: The role of dispersive forces in chiral discrimination. *J. Phys. Chem. A* **102**, 128–137 (1998).
55. M. Saeki, S.-i. Ishiuchi, M. Sakai, and M. Fujii, Structure of the jet-cooled 1-naphthol dimer studied by IR dip spectroscopy: Cooperation between the π–π interaction and the hydrogen bonding. *J. Phys. Chem. A* **111**, 1001–1005 (2007).
56. K. E. Riley and P. Hobza, Assessment of the MP2 method, along with several basis sets, for the computation of interaction energies of biologically relevant hydrogen bonded and dispersion bound complexes. *J. Phys. Chem. A* **111**, 8257–8263 (2007).
57. A. D. Boese, J. M. L. Martin, and W. Klopper, Basis set limit coupled cluster study of H-bonded systems and assessment of more approximate methods. *J. Phys. Chem. A* **111**, 11122–11133 (2007).
58. C. Emmeluth, V. Dyczmons, and M. A. Suhm, Tuning the hydrogen bond donor/acceptor isomerism in jet-cooled mixed dimers of aliphatic alcohols. *J. Phys. Chem. A* **110**, 2906–2915 (2006).
59. T. Suzuki, The hydration of glucose: The local configurations in sugar-water hydrogen bonds. *Phys. Chem. Chem. Phys.* **10**, 96–105 (2008).
60. A. Karpfen, Cooperativity effects in hydrogen bonding. *Adv. Chem. Phys.* **123**, 469–510 (2002).
61. M. Weimann, M. Fárník, and M. A. Suhm, Cooperative and anticooperative mixed trimers of HCl and methanol. *J. Mol. Struct.* **790**, 18–26 (2006).
62. M. A. Suhm and D. J. Nesbitt, Potential surfaces and dynamics of weakly bound trimers: Perspectives from high resolution IR spectroscopy. *Chem. Soc. Rev.* **24**, 45–54 (1995).
63. J. Demaison, M. Herman, and J. Lievin, The equilibrium OH bond length. *Mol. Phys.* **26**, 391–420 (2007).
64. J. R. Dixon, W. O. George, F. Hossain, R. Lewis, and J. M. Price, Hydrogen-bonded forms of methanol: IR spectra and *ab initio* calculations. *J. Chem. Soc., Faraday Trans.* **93**, 3611–3618 (1997).
65. T. Häber, U. Schmitt, and M. A. Suhm, FTIR-spectroscopy of molecular clusters in pulsed supersonic slit-jet expansions. *Phys. Chem. Chem. Phys.* **1**, 5573–5582 (1999).
66. Bretta F. King and F. Weinhold, Structure and spectroscopy of $(HCN)_n$ clusters: Cooperative and electronic delocalization effects in C–H···N hydrogen bonding. *J. Chem. Phys.* **103**, 333–347 (1995).
67. M. Quack and M. A. Suhm, Potential energy hypersurfaces for hydrogen bonded clusters $(HF)_n$, in *Conceptual Perspectives in Quantum Chemistry*, Conceptual Trends in Quantum Chemistry, Vol. III, J.-L. Calais and E. S. Kryachko, ed., Kluwer, Dordrecht, 1997, pp. 415–463.
68. M. Quack, J. Stohner, and M. A. Suhm, Analytical three-body interaction potentials and hydrogen bond dynamics of hydrogen fluoride aggregates $(HF)_n$, $n \geq 3$. *J. Mol. Struct.* **599**, 381–425 (2001).

69. T. N. Wassermann, P. Zielke, J. J. Lee, C. Cézard, and M. A. Suhm, Structural preferences, argon nanocoating, and dimerization of *n*-alkanols as revealed by OH stretching spectroscopy in supersonic jets. *J. Phys. Chem. A* **111**, 7437–7448 (2007).

70. M. Rozenberg, A. Loewenschuss, and Y. Marcus, An empirical correlation between stretching vibration redshift and hydrogen bond length. *Phys. Chem. Chem. Phys.* **2**, 2699–2702 (2000).

71. R. M. Badger and S. H. Bauer, Spectroscopic study of the hydrogen bond. II. The shift of the O–H vibrational frequency in the formation of the hydrogen bond. *J. Chem. Phys.* **5**, 839–851 (1937).

72. C. Cézard, C. A. Rice, and M. A. Suhm, OH-stretching redshifts in bulky hydrogen-bonded alcohols: Jet spectroscopy and modeling. *J. Phys. Chem. A* **110**, 9839–9848 (2006).

73. J. M. Lopez, F. Männle, I. Wawer, G. Buntkowsky, and H.-H. Limbach, NMR studies of double proton transfer in hydrogen bonded cyclic N,N'-diarylformamidine dimers: Conformational control, kinetic HH/HD/DD isotope effects and tunneling. *Phys. Chem. Chem. Phys.* **9**, 4498–4513 (2007).

74. M. N. Slipchenko, K. E. Kuyanov, B. G. Sartakov, and A. F. Vilesov, Infrared intensity in small ammonia and water clusters. *J. Chem. Phys.* **124**, 241101 (2006).

75. R. A. Provencal, J. B. Paul, K. Roth, C. Chapo, R. N. Casaes, R. J. Saykally, G. S. Tschumper, and H. F. Schaefer III, Infrared cavity ringdown spectroscopy of methanol clusters: Single donor hydrogen bonding. *J. Chem. Phys.* **110**, 4258–4267 (1999).

76. T. Scharge, T. Häber, and M. A. Suhm, Quantitative chirality synchronization in trifluoroethanol dimers. *Phys. Chem. Chem. Phys.* **8**, 4664–4667 (2006).

77. P. Zielke and M. A. Suhm, Concerted proton motion in hydrogen-bonded trimers: A spontaneous Raman scattering perspective. *Phys. Chem. Chem. Phys.* **8**, 2826–2830 (2006).

78. M. Fárník and D. J. Nesbitt, Intramolecular energy transfer between oriented chromophores: High-resolution infrared spectroscopy of HCl trimer. *J. Chem. Phys.* **121**, 12386–12395 (2004).

79. M. Quack, U. Schmitt, and M. A. Suhm, FTIR spectroscopy of hydrogen fluoride clusters in synchronously pulsed supersonic jets: Isotopic isolation, substitution and 3-D condensation. *Chem. Phys. Lett.* **269**, 29–38 (1997).

80. C. Emmeluth, V. Dyczmons, T. Kinzel, P. Botschwina, M. A. Suhm, and M. Yáñez, Combined jet relaxation and quantum chemical study of the pairing preferences of ethanol. *Phys. Chem. Chem. Phys.* **7**, 991–997 (2005).

81. H. L. Fang and D. A. C. Compton, Vibrational overtones of gaseous alcohols. *J. Phys. Chem.* **92**, 6518–6527 (1988).

82. D. Rueda, O. V. Boyarkin, T. R. Rizzo, I. Mukhopadhyay, and D. S. Perry, Torsion–rotation analysis of OH stretch overtone-torsion combination bands in methanol. *J. Chem. Phys.* **116**, 91–100 (2002).

83. P. Maksyutenko, O. V. Boyarkin, T. R. Rizzo, and D. S. Perry, Conformational dependence of intramolecular vibrational redistribution in methanol. *J. Chem. Phys.* **126**, 044311, (2007).

84. W. A. P. Luck and W. Ditter, Die Assoziation der Alkohole bis in überkritische Bereiche. *Ber. Bunsenges. Phys. Chem.* **72**, 365–492 (1968).

85. T. Di Paolo, C. Bourdéron, and C. Sandorfy, Model calculations on the influence of mechanical and electrical anharmonicity on infrared intensities: Relation to hydrogen bonding. *Can. J. Chem.* **50**, 3161–3166 (1972).

86. S. A. Nizkorodov, M. Ziemkiewicz, D. J. Nesbitt, and A. E. W. Knight, Overtone spectroscopy of H_2O clusters in the $v_{OH} = 2$ manifold: Infrared–ultraviolet vibrationally mediated dissociation studies. *J. Chem. Phys.* **122**, 194316 (2005).

87. L. England-Kretzer and W. A. P. Luck, Band analysis of CH_3OH and CH_3OD H-bond complexes in the first overtone region. *J. Mol. Struct.* **348**, 373–376 (1995).

88. J. P. Perchard and Z. Mielke, Anharmonicity and hydrogen bonding I. A near-infrared study of methanol trapped in nitrogen and argon matrices. *Chem. Phys.* **264**, 221–234 (2001).

89. T. Scharge, D. Luckhaus, and M. A. Suhm, Observation and quantification of the hydrogen bond effect on O–H overtone intensities in an alcohol dimer. *Chem. Phys.* **346**, 167–175 (2008).

90. J. T. Farrell, Jr., M. A. Suhm, and D. J. Nesbitt, Breaking symmetry with hydrogen bonds: Vibrational predissociation and isomerization dynamics in HF–DF and DF–HF isotopomers. *J. Chem. Phys.* **104**, 9313–9331 (1996).

91. J. P. I. Hearn, R. V. Cobley, and B. J. Howard, High-resolution spectroscopy of induced chiral dimers: A study of the dimers of ethanol by Fourier transform microwave spectroscopy. *J. Chem. Phys.* **123**, 134324 (2005).

92. P. Zielke and M. A. Suhm, Raman jet spectroscopy of formic acid dimers: Low frequency vibrational dynamics and beyond. *Phys. Chem. Chem. Phys.* **9**, 4528–4534 (2007).

93. R. Wugt Larsen and M. A. Suhm, Cooperative organic hydrogen bonds: The librational modes of cyclic methanol clusters. *J. Chem. Phys.* **125**, 154314 (2006).

94. M. Ehbrecht and F. Huisken, Vibrational spectroscopy of ethanol molecules and complexes selectively prepared in the gas phase and adsorbed on large argon clusters. *J. Phys. Chem. A* **101**, 7768–7777 (1997).

95. S. Coussan, Y. Boutellier, J. P. Perchard, and W. Q. Zheng, Rotational isomerism of ethanol and matrix isolation infrared spectroscopy. *J. Phys. Chem. A* **102**, 5789–5793 (1998).

96. U. Buck and I. Ettischer, Vibrational predissociation spectra of size-selected methanol clusters: New experimental results. *J. Chem. Phys.* **108**, 33–38 (1998).

97. F. Huisken and M. Staemmler, Infrared spectroscopy of methanol clusters adsorbed on large Ar_x host clusters. *J. Chem. Phys.* **98**, 7680–7691 (1993).

98. U. Buck and F. Huisken, Infrared spectroscopy of size-selected water and methanol clusters. *Chem. Rev.* **100**, 3863–3890 (2000).

99. C. J. Gruenloh, G. M. Florio, J. R. Carney, F. C. Hagemeister, and T. S. Zwier, C–H stretch modes as a probe of H-bonding in methanol-containing clusters. *J. Phys. Chem. A* **103**, 496–502 (1999).

100. S. Jarmelo, N. Maiti, V. Anderson, P. R. Carey, and R. Fausto, C_α–H bond-stretching frequency in alcohols as a probe of hydrogen-bonding strength: A combined vibrational spectroscopic and theoretical study of *n*-[1-D]propanol. *J. Phys. Chem. A* **109**, 2069–2077 (2005).

101. C. R. Quade, A note on internal rotation–rotation interactions in ethyl alcohol. *J. Mol. Spectrosc.* **203**, 200–202 (2000).

102. A. Maeda, F. C. De Lucia, E. Herbst, J. C. Pearson, J. Riccobono, E. Trosell, and R. K. Bohn, The millimeter- and submillimeter-wave spectrum of the Gt conformer of *n*-propanol (*n*-$CH_3CH_2CH_2OH$). *Astrophys. J. Suppl. Ser.* **162**, 428–435 (2006). See also abstract RI14, 61. *Mol. Spectr. Symp.*

103. S. Coussan, M. E. Alikhani, J. P. Perchard, and W. Q. Zheng, Infrared-induced isomerization of ethanol dimers trapped in argon and nitrogen matrices: Monochromatic irradiation experiments and DFT calculations. *J. Phys. Chem. A* **104**, 5475–5483 (2000).

104. A. Trivella, S. Coussan, T. Chiavassa, P. Theulé, P. Roubin, and C. Manca, Comparative study of structure and photo-induced reactivity of malonaldehyde and acetylacetone isolated in nitrogen matrices. *Low Temp. Phys.* **32**, 1042–1049 (2006).

105. R. D. Astumian, Design principles for Brownian molecular machines: How to swim in molasses and walk in a hurricane. *Phys. Chem. Chem. Phys.* **9**, 5067–5083 (2007).

106. M. V. Vener and J. Sauer, Vibrational spectra of the methanol tetramer in the OH stretch region. Two cyclic isomers and concerted proton tunneling. *J. Chem. Phys.* **114**, 2623–2628 (2001).

107. B. Fehrensen, D. Luckhaus, M. Quack, M. Willeke, and T. R. Rizzo, *Ab initio* calculations of mode selective tunneling dynamics in $^{12}CH_3OH$ and $^{13}CH_3OH$. *J. Chem. Phys.* **119**, 5534–5544 (2003).

108. D. Sabo, Z. Bačić, S. Graf, and S. Leutwyler, Four-dimensional model calculation of torsional levels of cyclic water tetramer. *J. Chem. Phys.* **109**, 5404–5419 (1998).

109. R. Berger, M. Quack, A. Sieben, and M. Willeke, Parity-violating potentials for the torsional motion of methanol (CH_3OH) and its isotopomers (CD_3OH, (CH_3OH)–C-13, CH_3OD, CH_3OT, CHD_2OH, and CHDTOH). *Helv. Chim. Acta* **86**, 4048–4060 (2003).

110. J. Paul, I. Hearn, and B. J. Howard, Chiral recognition in a single molecule: A study of homo and heterochiral butan-2,3,-diol by Fourier transform microwave spectroscopy. *Mol. Phys.* **105**, 825–839 (2007).

111. N. Borho and M. A. Suhm, Glycidol dimer: Anatomy of a molecular handshake. *Phys. Chem. Chem. Phys.* **4**, 2721–2732 (2002).

112. A. Al Rabaa, K. LeBarbu, F. Lahmani, and A. Zehnacker-Rentien, Van der Waals complexes between chiral molecules in a supersonic jet: A new spectroscopic method for enantiomeric discrimination. *J. Phys. Chem. A* **101**, 3273–3278 (1997).

113. K. Le Barbu-Debus, F. Lahmani, A. Zehnacker-Rentien, N. Guchhait, S. S. Panja, and T. Chakraborty, Fluorescence spectroscopy of jet-cooled chiral $(+/-)$-indan-1-ol and its cluster with $(+/-)$-methyl- and ethyl-lactate. *J. Chem. Phys.* **125**, 174305 (2006).

114. R. S. Cahn, Sir Christopher Ingold, and V. Prelog, Spezifikation der molekularen Chiralität. *Angew. Chem.* **78**, 413–447 (1966).

115. N. Borho, Diploma Thesis, Göttingen, 2001.

116. M. A. Czarnecki, Near-infrared spectroscopic study of hydrogen bonding in chiral and racemic octan-2-ol. *J. Phys. Chem. A* **107**, 1941–1944 (2003).

117. A. K. King and B. J. Howard, A microwave study of the hetero-chiral dimer of butan-2-ol. *Chem. Phys. Lett.* **348**, 343–349 (2001).

118. M. Speranza, Chiral clusters in the gas phase. *Adv. Phys. Org. Chem.* **39**, 147–281 (2004).

119. A. Latini, M. Satta, A. Giardini Guidoni, S. Piccirillo, and M. Speranza, Short-range interactions within molecular complexes formed in supersonic beams: Structural effects and chiral discrimination. *Chem. Eur. J.* **6**, 1042–1049 (2000).

120. K. Le Barbu, F. Lahmani, and A. Zehnacker-Rentien, Formation of hydrogen-bonded structures in jet-cooled complexes of a chiral chromophore studied by IR/UV double resonance spoctroscopy: Diastereomeric complexes of $\pm$-2-naphthyl-1-ethanol with $\pm$-2-amino-1-propanol. *J. Phys. Chem. A* **106**, 6271–6278 (2002).

121. N. Seurre, J. Sepioł, Katia Le Barbu-Debus, F. Lahmani, and A. Zehnacker-Rentien, The role of chirality in the competition between inter- and intramolecular hydrogen bonds: jet-cooled van der Waals complexes of $(\pm)$2-naphthyl-1-ethanol with $(\pm)$1-amino-2-propanol and $(\pm)$2-amino-1-butanol. *Phys. Chem. Chem. Phys.* **6**, 2867–2877 (2004).

122. T. B. Adler, N. Borho, M. Reiher, and M. A. Suhm, Chirality-induced switch in hydrogen-bond topology: Tetrameric methyl lactate clusters in the gas phase. *Angew. Chem. Int. Ed.* **45**, 3440–3445 (2006).

123. R. Graham Cooks, D. Zhang, K. J. Koch, F. C. Gozzo, and M. N. Eberlin, Chiroselective self-directed octamerization of serine: Implications for homochirogenesis. *Anal. Chem.* **73**, 3646–3655 (2001).

124. U. Mazurek, Some more aspects of formation and stability of the protonated serine octamer cluster. *Eur. J. Mass Spectrom.* **12**, 63–70 (2006).

125. N. Borho and M. A. Suhm, Self-organization of lactates in the gas phase. *Org. Biomol. Chem.* **1**, 4351–4358 (2003).

126. N. Seurre, K. Le Barbu-Debus, F. Lahmani, A. Zehnacker-Rentien, N. Borho, and M. A. Suhm, Chiral recognition between lactic acid derivatives and an aromatic alcohol in a supersonic expansion: Electronic and vibrational spectroscopy. *Phys. Chem. Chem. Phys.* **8**, 1007–1016 (2006).

127. A. Zehnacker and M. A. Suhm, Chirality recognition between neutral molecules in the gas phase. *Angew. Chem. Int. Ed.* **47**, 6970–6992 (2008).

128. N. Borho and Y. Xu, Molecular recognition in 1:1 hydrogen-bonded complexes of oxirane and *trans*-2,3-dimethyloxirane with ethanol: A rotational spectroscopic and *ab initio* study. *Phys. Chem. Chem. Phys.* **9**, 4514–4520 (2007).

129. T. Goldstein, M. S. Snow, and B. J. Howard, Intramolecular hydrogen bonding in chiral alcohols: The microwave spectrum of the chloropropanols. *J. Mol. Spectrosc.* **236**, 1–10 (2006).

130. T. Scharge, C. Emmeluth, Th. Häber, and M. A. Suhm, Competing hydrogen bond topologies in 2-fluoroethanol dimer. *J. Mol. Struct.* **786**, 86–95 (2006).

131. N. Solcà and O. Dopfer, Hydrogen-bonded networks in ethanol proton wires: IR spectra of $(EtOH)_q H^+$-L_n clusters ($L = Ar/N_2, q \leq 4, n \leq 5$). *J. Phys. Chem. A* **109**, 6174–6186 (2005).

132. T. D. Frigden, L. MacAleese, T. B. McMahon, J. Lemaire, and P. Maitre, Gas phase infrared multiple-photon dissociation spectra of methanol, ethanol and propanol proton-bound dimers, protonated propanol and the propanol/water proton-bound dimer. *Phys. Chem. Chem. Phys.* **8**, 955–966 (2006).

133. N. Uras-Aytemiz, J. P. Devlin, J. Sadlej, and V. Buch, HCl solvation at the surface and within methanol clusters/nanoparticles II: Evidence for molecular wires. *J. Phys. Chem. B* **110**, 21751–21763 (2006).

134. J. M. Lisy, Spectroscopy and structure of solvates alkali-metal ions. *Int. Rev. Phys. Chem.* **16**, 267–289 (1997).

135. C. A. Corbett, T. J. Martinez, and J. M. Lisy, Solvation of the fluoride anion by methanol. *J. Phys. Chem. A* **106**, 10015–10021 (2002).

136. W. H. Robertson, K. Karapetian, P. Ayotte, K. D. Jordan, and M. A. Johnson, Infrared predissociation spectroscopy of $I^- \cdots (CH_3OH)_n, n = 1, 2$: Cooperativity in asymmetric solvation. *J. Chem. Phys.* **116**, 4853–4857 (2002).

137. A. Kammrath, G. B. Griffin, J. R. R. Verlet, R. M. Young, and D. M. Neumark, Time-resolved photoelectron imaging of large anionic methanol clusters: $(Methanol)_n^-$($n \sim 145$–535). *J. Chem. Phys.* **126**, 244306 (2007).

138. Y. Ferro, A. Allouche, and V. Kempter, Electron solvation by highly polar molecules: Density functional theory study of atomic sodium interaction with water, ammonia, and methanol. *J. Chem. Phys.* **120**, 8683–8691 (2004).

139. Y. Liu, Corey A. Rice, and M. A. Suhm, Torsional isomers in methylated aminoethanols: A jet-FTIR study. *Can. J. Chem.* **82**, 1006–1012 (2004).

140. B. C. Ibănescu, O. May, A. Monney, and M. Allan, Electron-induced chemistry of alcohols. *Phys. Chem. Chem. Phys.* **9**, 3163–3173 (2007).

141. P. C. Blainey and P. J. Reid, FTIR studies of intermolecular hydrogen bonding in halogenated ethanols. *Spectrochim. Acta Part A* **57**, 2763–2774 (2001).

142. M. A. F. H. van den Broek, H.-K. Nienhuys, and H. J. Bakker, Vibrational dynamics of the C—O stretch vibration in alcohols. *J. Chem. Phys.* **114**, 3182–3186 (2001).

143. C. L. Lugez, F. J. Lovas, J. T. Hougen, and N. Ohashi, Global analysis of a-, b-, and c-type transitions involving tunneling components of $K = 0$ and 1 states of the methanol dimer. *J. Mol. Spectrosc.* **194**, 95–112 (1999).

144. N. Borho and Y. Xu, Lock-and-key principle on a microscopic scale: The case of the propylene oxide–ethanol complex. *Angew. Chem. Int. Ed.* **46**, 2276–2279 (2007).

145. S. Melandri, P. G. Favero, and W. Caminati, Detection of the syn conformer of allyl alcohol by free jet microwave spectroscopy. *Chem. Phys. Lett.* **223**, 541–545 (1994).

146. L. H. Xu, G. T. Fraser, F. J. Lovas, R. D. Suenram, C. W. Gillies, H. E. Warner, and J. Z. Gillies, The microwave-spectrum and OH internal-rotation dynamics of gauche-2,2,2-trifluoroethanol. *J. Chem. Phys.* **103**, 9541–9548 (1995).

147. H. Møllendal, Structural and conformational properties of 1,1,1-trifluoro-2-propanol investigated by microwave spectroscopy and quantum chemical calculations. *J. Phys. Chem. A* **109**, 9488–9493 (2005).

148. K. O. Douglass, J. E. Johns, P. M. Nair, G. G. Brown, F. S. Rees, and B. H. Pate, Applications of Fourier transform microwave (FTMW) detected infrared-microwave double-resonance spectroscopy to problems in vibrational dynamics. *J. Mol. Spectrosc.* **239**, 29–40 (2006).

149. A. Westphal, C. Jacoby, C. Ratzer, A. Reichelt, and M. Schmitt, Determination of the intermolecular geometry of the phenol-methanol cluster. *Phys. Chem. Chem. Phys.* **5**, 4114–4122 (2003).

150. J. T. Yi and D. W. Pratt, Rotationally resolved electronic spectroscopy of tryptophol in the gas phase. *Phys. Chem. Chem. Phys.* **7**, 3680–3684 (2005).

151. D. J. Nesbitt, High-resolution, direct infrared laser absorption spectroscopy in slit supersonic jets: Intermolecular forces and unimolecular vibrational dynamics in clusters. *Annu. Rev. Phys. Chem.* **45**, 367–399 (1994).

152. D. Luckhaus, M. Quack, U. Schmitt, and M. A. Suhm, On FTIR spectroscopy in asynchronously pulsed supersonic jet expansions and on the interpretation of stretching spectra of HF clusters. *Ber. Bunsenges. Phys. Chem.* **99**, 457–468 (1995).

153. C. A. Rice, N. Borho, and M. A. Suhm, Dimerization of pyrazole in slit jet expansions. *Z. Phys. Chem.* **219**, 379–388 (2005).

154. N. Borho, M. A. Suhm, K. Le Barbu-Debus, and A. Zehnacker, Intra- vs. intermolecular hydrogen bonding: Dimers of alpha-hydroxyesters with methanol. *Phys. Chem. Chem. Phys.* **8**, 4449–4460 (2006).

155. T. N. Wassermann, D. Luckhaus, S. Coussan, and M. A. Suhm, Proton tunneling estimates for malonaldehyde vibrations from supersonic jet and matrix quenching experiments. *Phys. Chem. Chem. Phys.* **8**, 2344–2348 (2006).

156. Y. Liu, M. Weimann, and M. A. Suhm, Extension of panoramic cluster jet spectroscopy into the far infrared: Low frequency modes of methanol and water clusters. *Phys. Chem. Chem. Phys.* **6**, 3315–3319 (2004).

157. R. A. Provencal, R. N. Casaes, K. Roth, J. B. Paul, C. N. Chapo, R. J. Saykally, G. S. Tschumper, and H. F. Schaefer, Hydrogen bonding in alcohol clusters: A comparative study by infrared cavity ringdown laser absorption spectroscopy. *J. Phys. Chem. A* **104**, 1423–1429 (2000).

158. T. Häber, U. Schmitt, C. Emmeluth, and M. A. Suhm, Ragout-jet FTIR spectroscopy of cluster isomerism and cluster dynamics: From carboxylic acid dimers to N_2O nanoparticles. *Faraday*

Discuss. **118**, 331–359 (2001) + contributions to the discussion on pp. 53, 119, 174–175, 179–180, 304–309, 361–363, 367–370.

159. M. Herman, R. Georges, M. Hepp, and D. Hurtmans, High resolution Fourier transform spectroscopy of jet-cooled molecules. *Int. Rev. Phys. Chem.* **19**, 277–325 (2000).
160. M. Behrens, R. Fröchtenicht, M. Hartmann, J.-G. Siebers, U. Buck, and F. C. Hagemeister, Vibrational spectroscopy of methanol and acetonitrile clusters in cold helium droplets. *J. Chem. Phys.* **111**, 2436–2443 (1999).
161. W. Richter and D. Schiel, Raman spectrometric investigation of the molecular structure of alcohols; Conformational dynamics of ethanol. *Ber. Bunsenges. Phys. Chem.* **85**, 548–552 (1981).
162. B. Maté, I. A. Graur, T. Elizarova, I. Chirokov, G. Tejeda, J. M. Fernández, and S. Montero, Experimental and numerical investigation of an axisymmetric supersonic jet. *J. Fluid Mech.* **426**, 177–197 (2001).
163. J. M. Fernández, G. Tejeda, A. Ramos, B. J. Howard, and S. Montero, Gas-phase Raman spectrum of NO dimer, *J. Mol. Spec.* **194**, 278–280 (1999).
164. G. Tejeda, J. M. Fernández, S. Montero, D. Blume, and J. P. Toennies, Raman spectroscopy of small para-H_2 clusters formed in cryogenic free jets. *Phys. Rev. Lett.* **92**, 223401–1 (2004).
165. P. M. Felker, P. M. Maxton, and M. W. Schaeffer, Nonlinear Raman studies of weakly bound complexes and clusters in molecular beams. *Chem. Rev.* **94**, 1787–1805 (1994).
166. T. Ebata, T. Watanabe, and N. Mikami, Evidence for the cyclic form of phenol trimer: Vibrational spectroscopy of the OH stretching vibrations of jet-cooled phenol dimer and trimer, *J. Phys. Chem.* **99**, 5761–5764 (1995).
167. Y. Matsuda, M. Hachiya, A. Fujii, and N. Mikami, Stimulated Raman spectroscopy combined with vacuum ultraviolet photoionization: Application to jet-cooled methanol clusters as a new vibrational spectroscopic method for size-selected species in the gas phase. *Chem. Phys. Lett.* **442**, 217–219 (2007).
168. M. Maroncelli, G. A. Hopkins, J. W. Nibler, and T. R. Dyke, Coherent Raman and infrared spectroscopy of HCN complexes in free jet expansions and in equilibrium samples. *J. Phys. Chem.* **83**, 2129–2146 (1985).
169. A. Furlan, S. Wülfert, and S. Leutwyler, CARS spectra of the HCl dimer in supersonic jets. *Chem. Phys. Lett.* **153**, 291–295 (1988).
170. M. G. Giorgini, Raman noncoincidence effect: A spectroscopic manifestation of the intermolecular vibrational coupling in dipolar molecular liquids. *Pure Appl. Chem.* **76**, 157–169 (2004).
171. M. Paolantoni, P. Sassi, A. Morresi, and R. S. Cataliotti, Raman noncoincidence effect on OH stretching profiles in liquid alcohols. *J. Raman Spectr.* **37**, 528–537 (2006).
172. Y. J. Hu, H. B. Fu, and E. R. Bernstein, Infrared plus vacuum ultraviolet spectroscopy of neutral and ionic methanol monomers and clusters: New experimental results. *J. Chem. Phys.* **125**, 154306 (2006).
173. F. Huisken, M. Kaloudis, M. Koch, and O. Werhahn, Experimental study of the O–H ring vibrations of the methanol trimer. *J. Chem. Phys.* **105**, 8965–8968 (1996).
174. C. Steinbach, M. Fárník, I. Ettischer, J. Siebers, and U. Buck, Isomeric transitions in size-selected methanol hexamers probed by OH-stretch spectroscopy. *Phys. Chem. Chem. Phys.* **8**, 2752–2756 (2006).
175. B. Brutschy, The structure of microsolvated benzene derivatives and the role of aromatic substituents. *Chem. Rev.* **100**, 3891–3920 (2000).

176. Y. Nosenko, A. Kyrychenko, R. P. Thummel, J. Waluk, B. Brutschy, and J. Herbich, Fluorescence quenching in cyclic hydrogen-bonded complexes of 1*H*-pyrrolo[3,2-*h*]quinoline with methanol: Cluster size effect. *Phys. Chem. Chem. Phys.* **9**, 3276–3285 (2007).

177. Y. Nosenko, M. Kunitski, R. P. Thummel, A. Kyrychenko, J. Herbich, J. Waluk, C. Riehn, and B. Brutschy, Detection and structural characterization of clusters with ultrashort-lived electronically excited states: IR absorption detected by femtosecond multiphoton ionization. *J. Am. Chem. Soc.* **128**, 10000 (2006).

178. N. Guchhait, T. Ebata, and N. Mikami, Discrimination of rotamers of aryl alcohol homologues by infrared–ultraviolet double-resonance spectroscopy in a supersonic jet. *J. Am. Chem. Soc.* **121**, 5705–5711 (1999).

179. M. Mons, E. G. Robertson, and J. P. Simons, Intra- and intermolecular π-type hydrogen bonding in aryl alcohols: UV and IR–UV ion dip spectroscopy. *J. Phys. Chem. A* **104**, 1430–1437 (2000).

180. R. N. Pribble, F. C. Hagemeister, and T. S. Zwier, Resonant ion-dip infrared spectroscopy of benzene-$(\text{methanol})_m$ clusters with $m = 1$–6. *J. Chem. Phys.* **106**, 2145–2157 (1997).

181. Y. Matsumoto, T. Ebata, and N. Mikami, Structure and photoinduced excited state keto-enol tautomerization of 7-hydroxyquinoline-$(CH_3OH)_n$ clusters. *J. Phys. Chem. A* **106**, 5591–5599 (2002).

182. C. Plützer, C. Jacoby, and M. Schmitt, Internal rotation and intermolecular vibrations of the phenol–methanol cluster: A comparison of spectroscopic results and *ab initio* theory. *J. Phys. Chem. A* **106**, 3998–4004 (2002).

183. V. A. Shubert and T. S. Zwier, IR–IR–UV hole-burning: Conformation specific IR spectra in the face of UV spectral overlap. *J. Phys. Chem. A* **111**, 13283–13286 (2007).

184. Y. J. Hu, H. B. Fu, and E. R. Bernstein, Infrared plus vacuum ultraviolet spectroscopy of neutral and ionic ethanol monomers and clusters. *J. Chem. Phys.* **125**, 154305 (2006).

185. Y. J. Hu, H. B. Fu, and E. R. Bernstein, IR plus vacuum ultraviolet spectroscopy of neutral and ionic organic acid monomers and clusters: Propanoic acid. *J. Chem. Phys.* **125**, 184309 (2006).

186. M. Abu-samha, K. J. Borve, J. Harnes, and H. Bergersen, What can C1s photoelectron spectroscopy tell about structure and bonding in clusters of methanol and methyl chloride. *J. Phys. Chem. A* **111**, 8903–8909 (2007).

187. J. M. Wang, P. Cieplak, and P. A. Kollmann, How well does a restrained electrostatic potential (RESP) model perform in calculating conformational energies of organic and biological molecules? *J. Comput. Chem.* **21**, 1049–1074 (2000).

188. W. T. M. Mooij, F. B. van Duijneveldt, J. G. C. M. van-Duijneveldt–van de Rijdt, and Bouke P. van Eijck, Transferable *ab initio* intermolecular potentials. 1. derivation from methanol dimer and trimer calculations. *J. Phys. Chem. A* **103**, 9872–9882 (1999).

189. U. Buck, J.-G. Siebers, and R. J. Wheatley, Structure and vibrational spectra of methanol clusters from a new potential model. *J. Chem. Phys.* **108**, 20–32 (1998).

190. M. Karplus, Molecular dynamics of biological macromolecules: A brief history and perspective. *Biopolymers* **68**, 350–358 (2003).

191. M. Gerhards, K. Beckmann, and K. Kleinermanns, Vibrational analysis of phenol(methanol)$_1$. *Z. Phys. D* **29**, 223–229 (1994).

192. H.-J. Werner, F. R. Manby, and P. J. Knowles, Fast linear scaling second-order Møller–Plesset perturbation theory (MP2) using local and density fitting approximations. *J. Chem. Phys.* **118**, 8149–8160 (2003).

193. M. J. Frisch, G. W. Trucks, H. B. Schlegel, G. E. Scuseria, M. A. Robb, J. R. Cheeseman, J. A. Montgomery, Jr., T. Vreven, K. N. Kudin, J. C. Burant, J. M. Millam, S. S. Iyengar, J. Tomasi, V. Barone, B. Mennucci, M. Cossi, G. Scalmani, N. Rega, G. A. Petersson, H. Nakatsuji,

M. Hada, M. Ehara, K. Toyota, R. Fukuda, J. Hasegawa, M. Ishida, T. Nakajima, Y. Honda, O. Kitao, H. Nakai, M. Klene, X. Li, J. E. Knox, H. P. Hratchian, J. B. Cross, C. Adamo, J. Jaramillo, R. Gomperts, R. E. Stratmann, O. Yazyev, A. J. Austin, R. Cammi, C. Pomelli, J. W. Ochterski, P. Y. Ayala, K. Morokuma, G. A. Voth, P. Salvador, J. J. Dannenberg, V. G. Zakrzewski, S. Dapprich, A. D. Daniels, M. C. Strain, O. Farkas, D. K. Malick, A. D. Rabuck, K. Raghavachari, J. B. Foresman, J. V. Ortiz, Q. Cui, A. G. Baboul, S. Clifford, J. Cioslowski, B. B. Stefanov, G. Liu, A. Liashenko, P. Piskorz, I. Komaromi, R. L. Martin, D. J. Fox, T. Keith, M. A. Al-Laham, C. Y. Peng, A. Nanayakkara, M. Challacombe, P. M. W. Gill, B. Johnson, W. Chen, M. W. Wong, C. Gonzalez, and J. A. Pople, Gaussian 03, Revisions B.04 and C.02., Gaussian Inc., Pittsburgh PA, 2003.

194. C. Maerker, P. von Ragué Schleyer, R. Liedl, T.-K. Ha, M. Quack, and M. A. Suhm, A critical analysis of electronic density functionals for structural, energetic, dynamic and magnetic properties of hydrogen fluoride clusters. *J. Comput. Chem.* **18**, 1695–1719 (1997).
195. O. Mó, M. Yáñez, and J. Elguero, Study of the methanol trimer potential energy surface. *J. Chem. Phys.* **107**, 3592–3601 (1997).
196. F. C. Hagemeister, C. J. Gruenloh, and T. S. Zwier, Density functional theory calculations of the structures, binding energies, and infrared spectra of methanol clusters. *J. Phys. Chem. A* **102**, 82–94 (1998).
197. S. L. Boyd and R. J. Boyd, A density functional study of methanol clusters. *J. Chem. Theory Comput.* **3**, 54–61 (2007).
198. T. Schwabe and S. Grimme, Double-hybrid density functionals with long-range dispersion corrections: Higher accuracy and extended applicability. *Phys. Chem. Chem. Phys.* **9**, 3397–3406 (2007).
199. A. Bleiber and J. Sauer, The vibrational frequency of the donor OH group in the H-bonded dimers of water, methanol and silanol. *Ab initio* calculations including anharmonicities. *Chem. Phys. Lett.* **238**, 243–252 (1995).
200. T. H. Dunning, Jr, A road map for the calculation of molecular binding energies. *J. Phys. Chem. A* **104**, 9062–9080 (2000).
201. E. M. Mas, R. Bukowski, and K. Szalewicz, *Ab initio* three-body interactions for water. I. Potential and structure of water trimer. *J. Chem. Phys.* **118**, 4386–4403 (2003).
202. W. Klopper, M. Quack, and M. A. Suhm, HF dimer: Empirically refined analytical potential energy and dipole hypersurfaces from *ab initio* calculations. *J. Chem. Phys.* **108**, 10096–10115 (1998).
203. D. J. Wales, J. P. K. Doye, M. A. Miller, P. N. Mortenson, and T. R. Walsh, Energy landscapes: From clusters to biomolecules. *Adv. Chem. Phys.* **115**, 1–111 (2000).
204. F. Schulz and B. Hartke, Structural information on alkali cation microhydration clusters from infrared spectra. *Phys. Chem. Chem. Phys.* **5**, 5021–5030 (2003).
205. C. Herrmann, J. Neugebauer, and M. Reiher, Finding a needle in a haystack: direct determination of vibrational signatures in complex systems. *New J. Chem.* **31**, 818–831 (2007).
206. V. Barone, Anharmonic vibrational properties by a fully automated second-order perturbative approach. *J. Chem. Phys.* **122**, 014108 (2005).
207. S. K. Gregurick, J. H.-Y. Liu, D. A. Brant, and R. B. Gerber, Anharmonic vibrational self-consistent field calculations as an approach to improving force fields for monosaccharides. *J. Phys. Chem. B* **103**, 3476–3488 (1999).
208. J. M. Bowman, S. Carter, and X. C. Huang, MULTIMODE: a code to calculate rovibrational energies of polyatomic molecules. *Int. Rev. Phys. Chem.* **22**, 533–549 (2003).
209. X.-G. Wang and T. Carrington, Jr., Six-dimensional variational calculation of the bending energy levels of HF trimer and DF trimer. *J. Chem. Phys.* **115**, 9781–9796 (2001).

210. M. D. Coutinho-Neto, A. Viel, and U. Manthe, The ground state tunneling splitting of malonaldehyde: Accurate full dimensional quantum dynamics calculations. *J. Chem. Phys.* **121**, 9207–9210 (2004).

211. G. V. Mil'nikov, O. Kühn, and H. Nakamura, Ground-state and vibrationally assisted tunneling in the formic acid dimer. *J. Chem. Phys.* **123**, 074308 (2005).

212. J.-W. Handgraaf, E. J. Meijer, and M.-P. Gaigeot, Density-functional theory-based molecular simulation study of liquid methanol. *J. Chem. Phys.* **121**, 10111–10119 (2004).

213. G. S. Fanourgakis, Y. J. Shi, S. Consta, and R. H. Lipson, A spectroscopic and computer simulation study of butanol vapors. *J. Chem. Phys.* **119**, 6597–6608 (2003).

214. A. Serrallach, R. Meyer, and H. H. Günthard, Methanol and deuterated species: Infrared data, valence force field, rotamers, and conformation. *J. Mol. Spectrosc.* **52**, 94–129 (1974).

215. J. Florian, J. Leszczynski, B. G. Johnson, and L. Goodman, Coupled-cluster and density functional calculations of the molecular structure, infrared spectra, Raman spectra, and harmonic force constants for methanol. *Mol. Phys.* **91**, 439–447 (1977).

216. R. H. Hunt, W. N. Shelton, F. A. Flaherty, and W. B. Cook, Torsion–rotation energy levels and the hindering potential barrier for the excited vibrational state of the OH-stretch fundamental band ν_1 of methanol. *J. Mol. Spectrosc.* **192**, 277–293 (1998).

217. O. V. Boyarkin, T. R. Rizzo, and D. S. Perry, Intramolecular energy transfer in highly vibrationally excited methanol. II. Multiple time scales of energy redistribution. *J. Chem. Phys.* **110**, 11346–11358 (1999).

218. V. Venkatesan, A. Fujii, T. Ebata, and N. Mikami, Infrared and *ab initio* studies on 1,2,4,5-tetrafluorobenzene clusters with methanol and 2,2,2-trifluoroethanol: Presence and absence of an aromatic C─H$\cdots$O hydrogen bond. *J. Phys. Chem. A* **109**, 915–921 (2005).

219. G. S. Tschumper, J. M. Gonzales, and H. F. Schaefer III, Assignment of the infrared spectra of the methanol trimer. *J. Chem. Phys.* **111**, 3027–3034 (1999).

220. M. Mandado, A. M. Grana, and R. A. Mosquera, On the structures of the methanol trimer and their cooperative effects. *Chem. Phys. Lett.* **381**, 22–29 (2003).

221. W. F. Passchier, E. R. Klompmaker, and M. Mandel, Absorption spectra of liquid and solid methanol from 1000 to 100 cm^{-1}. *Chem. Phys. Lett.* **4**, 485–488 (1970).

222. J. R. Durig, C. B. Pate, Y. S. Li, and D. J. Antion, Far-infrared and Raman spectra of solid methanol and methanol-d_4. *J. Chem. Phys.* **54**, 4863–4870 (1971).

223. K. N. Woods and H. Wiedemann, The influence of chain dynamics on the far-infrared spectrum of liquid methanol. *J. Chem. Phys.* **123**, 134506 (2005).

224. P.-G. Jönsson, Hydrogen bond studies. CXIII. The crystal structure of ethanol at 87 K. *Acta Crystallogr.* **B32**, 232–235 (1976).

225. M. Rozenberg, A. Loewenschuss, and Y. Marcus, IR spectra and hydrogen bonding in ethanol crystals at 18–150 K. *Spectrochim. Acta Part A* **53**, 1969–1974 (1997).

226. A. J. Barnes and H. E. Hallam, Infrared cryogenic studies, part 5—Ethanol and ethanol-d in argon matrices. *Trans. Faraday Soc.* **66**, 1932–1940 (1970).

227. N. Nishi, S. Takahashi, M. Matsumoto, A. Tanaka, K. Muraya, T. Takamuku, and T. Yamaguchi, Hydrogen bonding cluster formation and hydrophobic solute association in aqueous solution of ethanol. *J. Phys. Chem.* **99**, 462–468 (1995).

228. M. Nedić, T. N. Wassermann, Z. Xue, P. Zielke, M. A. Suhm, Raman spectroscopic evidence for the most stable water/ethanol dimer and for the negative mixing energy in cold water/ethanol trimers. *Phys. Chem. Chem. Phys.* **10**, 5953–5956 (2008).

229. D. Spangenberg, P. Imhof, W. Roth, C. Janzen, and K. Kleinermanns, Phenol-(ethanol)$_1$ isomers studied by double-resonance spectroscopy and *ab initio* calculations. *J. Phys. Chem. A* **103**, 5918–5924 (1999).

230. B. T. G. Lutz and J. H. van der Maas, The sensorial potentials of the OH stretching mode. *J. Mol. Struct.* **436–437**, 213–231 (1997).

231. K. Ohno, H. Yoshida, H. Watanabe, T. Fujita, and H. Matsuura, Conformational study of 1-butanol by the combined use of vibrational spectroscopy and *ab initio* molecular orbital calculations. *J. Phys. Chem.* **98**, 6924–6930 (1994).

232. K. Kahn and T. C. Bruice, Focal-point conformational analysis of ethanol, propanol, and isopropanol. *ChemPhysChem* **6**, 487–495 (2005).

233. A. V. Bochenkova, M. A. Suhm, A. A. Granovsky, and A. V. Nemukhin, Hybrid diatomics-in-molecules-based quantum mechanical/molecular mechanical approach applied to the modeling of structures and spectra of mixed molecular clusters $Ar_n(HCl)_m$ and $Ar_n(HF)_m$. *J. Chem. Phys.* **120**, 3732–3743 (2004).

234. B. Lutz, R. Scherrenberg, and J. van der Maas, The associative behaviour of saturated alcohols with reference to the molecular structure in the OH proximity. An FT–IR temperature study. *J. Mol. Struct.* **175**, 233–238 (1988).

235. M. Saeki, S.-i. Ishiuchi, M. Sakai, and M. Fujii, Structure of 1-naphthol/alcohol clusters studied by IR dip spectroscopy and *ab initio* molecular orbital calculations. *J. Phys. Chem. A* **105**, 10045–10053 (2001).

236. D. T. Bowron, J. L. Finney, and A. K. Soper, The structure of pure tertiary butanol. *Mol. Phys.* **93**, 531–543 (1998).

237. D. T. Bowron and J. L. Finney, Association and dissociation of an aqueous amphiphile at elevated temperatures. *J. Phys. Chem. B* **111**, 9838–9852 (2007).

238. A. V. Iogansen and M. S. Rozenberg, Infrared bands of the OH (OD) group, hydrogen bonding, and special features of the structure of crystals of tert-butanol at 15–300 K. *J. Struct. Chem.* **30**, 76–83 (1989).

239. H. Serrano-Gonzáles, K. D. M. Harris, C. C. Wilson, A. E. Aliev, S. J. Kitchin, B. M. Kariuki, M. Bach-Vergés, C. Glidewell, E. J. MacLean, and W. W. Kagunya, Unravelling the disordered hydrogen bonding arrangement in solid triphenylmethanol. *J. Phys. Chem. B* **103**, 6215–6223 (1999).

240. F. Vanhouteghem, W. Pyckhout, C. Van Alsenoy, L. Van den Enden, and H. J. Geise, The molecular structure of gaseous allyl alcohol determined from electron diffraction, microwave, infrared and geometry-relaxed *ab-initio* data. *J. Mol. Struct.* **140**, 33–48 (1986).

241. A. Aspiala, T. Lotta, J. Murto, and M. Räsänen, IR-induced processes for allyl alcohol dimers involving an intermolecular OH . . . π bond in low-temperature matrices. *Chem. Phys. Lett.* **112**, 469–472 (1984).

242. T. Baba, T. Tanaka, I. Morino, K. M. T. Yamada, and K. Tanaka, Detection of the tunneling-rotation transitions of malonaldehyde in the submillimeter-wave region. *J. Chem. Phys.* **110**, 4131–4133 (1999).

243. C. Duan and D. Luckhaus, High resolution IR-diode laser jet spectroscopy of malonaldehyde. *Chem. Phys. Lett.* **391**, 129–133 (2004).

244. R. L. Redington and T. E. Redington, Implications of comparative spectral doublets observed for neon-isolated and gaseous tropolone(OH) and tropolone(OD). *J. Chem. Phys.* **122**, 124304, (2005).

245. C. Emmeluth, M. A. Suhm, and D. Luckhaus, A monomers-in-dimers model for carboxylic acid dimers. *J. Chem. Phys.* **118**, 2242–2255 (2003).

246. M. Schmitt, U. Henrichs, H. Müller, and K. Kleinermanns, Intermolecular vibrations of the phenol dimer revealed by spectral hole-burning and dispersed fluorescence spectroscopy. *J. Chem. Phys.* **103**, 9918–9928 (1995).

247. M. Schmitt, M. Böhm, C. Ratzer, D. Krügler, K. Kleinermanns, I. Kalkman, G. Berden, and W. Leo Meerts, Determining the intermolecular structure in the S_0 and S_1 states of the phenol dimer by rotationally resolved electronic spectroscopy. *ChemPhysChem* **7**, 1241–1249 (2006).

248. W. J. Middleton and R. V. Lindsey, Jr., Hydrogen bonding in fluoro alcohols. *J. Am. Chem. Soc.* **86**, 4948–4952 (1964).

249. A. Kovács and Z. Varga, Halogen acceptors in hydrogen bonding. *Coord. Chem. Rev.* **250**, 710–727 (2006).

250. J. D. Dunitz and R. Taylor, Organic fluorine hardly ever accepts hydrogen bonds. *Chemistry Eur. J.* **3**, 89–98 (1997).

251. R. D. Suenram, F. J. Lovas, and H. M. Pickett, Fluoromethanol: Synthesis, microwave spectrum, and dipole moment. *J. Mol. Spectrosc.* **119**, 446–455 (1986).

252. S. Andreades and D. C. England, α-haloalcohols. *J. Am. Chem. Soc.* **83**, 4670–4671 (1961).

253. J. M. Bakke, L. H. Bjerkeseth, T. E. C. L. Rønnow, and K. Steinsvoll, The conformation of 2-fluoroethanol—Is intramolecular hydrogen bonding important? *J. Mol. Struct.* **321**, 205–214 (1994).

254. P. Maienfisch and R. G. Hall, The importance of fluorine in the life science industry. *Chimia* **58**, 93–99 (2004).

255. J. W. Grate, Hydrogen-bond acidic polymers for chemical vapor sensing. *Chem. Rev.* **108**, 726–745 (2008).

256. J.-P. Bégué, D. Bonnet-Delpon, and B. Crousse, Fluorinated alcohols: A new medium for selective and clean reaction. *Synlett*, 18–29 (2004).

257. A. Berkessel and J. A. Adrio, Dramatic acceleration of olefin epoxidation in fluorinated alcohols: Activation of hydrogen peroxide by multiple H-bond networks. *J. Am. Chem. Soc.* **128**, 13412–13420 (2006).

258. M. Buck, Trifluoroethanol and colleagues: cosolvents come of age. recent studies with peptides and proteins. *Q. Rev. Biophys.* **31**, 297–355 (1998).

259. D. Roccatano, G. Colombo, M. Fioroni, and A. E. Mark, Mechanism by which 2,2,2-trifluoroethanol/water mixtures stabilize secondary-structure formation in peptides: A molecular dynamics study. *Proc. Natl. Acad. Sci. USA* **99**, 12179–12184 (2002).

260. A. Starzyk, W. Barber-Armstrong, M. Sridharan, and S. M. Decatur, Spectroscopic evidence for backbone desolvation of helical peptides by 2,2,2-trifluoroethanol: An isotope-edited FTIR study. *Biochemistry* **44**, 369–376 (2005).

261. K. O. Christe, J. Hegge, B. Hoge, and R. Haiges, Convenient access to trifluoromethanol. *Angew. Chem. Int. Ed.* **46**, 6155–6158 (2007).

262. M. Perttila, Vibrational-spectra and normal coordinate analysis of 2,2,2-trichloroethanol and 2,2,2-trifluoroethanol. *Spectrochim. Acta Part A* **35**, 585–592 (1978).

263. M. L. Senent, A. Perez-Ortega, A. Arroyo, and R. Domínguez-Gómez, Theoretical investigation of the torsional spectra of 2,2,2-trifluoroethanol. *Chem. Phys.* **266**, 19–32 (2001).

264. I. Bako, T. Radnai, and M. C. Bellissent-Funel, Investigation of structure of liquid 2,2,2-trifluoroethanol: Neutron diffraction, molecular dynamics, and *ab initio* quantum chemical study. *J. Chem. Phys.* **121**, 12472–12480 (2004).

265. H. L. Fang and R. L. Swofford, Molecular conformers in gas-phase ethanol: A temperature study of vibrational overtones. *Chem. Phys. Lett.* **105**, 5–11 (1984).

266. U. Erlekam, M. Frankowski, G. von Helden, and G. Meijer, Cold collisions catalyse conformational conversion. *Phys. Chem. Chem. Phys.* **9**, 3786–3789 (2007).

267. M. Fioroni, K. Burger, A. E. Mark, and D. Roccatano, A new 2,2,2-trifluoroethanol model for molecular dynamics simulations. *J. Phys. Chem. B* **104**, 12347–12354 (2000).

268. M. L. Senent, A. Nino, C. Munoz-Caro, Y. G. Smeyers, R. Dominguez-Gomez, and J. M. Orza, Theoretical study of the effect of hydrogen-bonding on the stability and vibrational spectrum of isolated 2,2,2-trifluoroethanol and its molecular complexes. *J. Phys. Chem. A* **106**, 10673–10680 (2002).

269. H. Schaal, T. Häber, and M. A. Suhm, Hydrogen bonding in 2-propanol: The effect of fluorination. *J. Phys. Chem. A* **104**, 265–274 (2000).

270. M. Fioroni, K. Burger, and D. Roccatano, Chiral discrimination in liquid 1,1,1-trifluoropropan-2-ol: A molecular dynamics study. *J. Chem. Phys.* **119**, 7289–7296 (2003).

271. T. J. Wallington, W. F. Schneider, I. Barnes, K. H. Becker, J. Sehested, and O. J. Nielsen, Stability and infrared spectra of mono-, di-, and trichloromethanol. *Chem. Phys. Lett.* **322**, 97–102 (2000).

272. M. Jackson and H. H. Mantsch, Halogenated alcohols as solvents for proteins: FTIR spectroscopic studies. *Biochim. Biophys. Acta* **1118**, 139–143 (1992).

273. V. Moulin, A. Schriver, L. Schriver-Mazzuoli, and P. Chaquin, Infrared spectrum of 2,2,2-trichloroethanol isolated in gas matrices. *Ab initio* optimization of conformers and potential energy calculations. *Chem. Phys. Lett.* **263**, 423–428 (1996).

274. N. Borho and M. A. Suhm, Tailor-made aggregates of α-hydroxy esters in supersonic jets. *Phys. Chem. Chem. Phys.* **6**, 2885–2890 (2004).

275. M. Fárník, M. Weimann, C. Steinbach, U. Buck, N. Borho, T. B. Adler, and M. A. Suhm, Size-selected methyl lactate clusters: Fragmentation and spectroscopic fingerprints of chiral recognition. *Phys. Chem. Chem. Phys.* **8**, 1148–1158 (2006).

276. R. Iwamoto, T. Matsuda, and H. Kusanagi, Contrast effect of hydrogen bonding on the acceptor and donor OH groups of intramolecularly hydrogen-bonded OH pairs in diols. *Spectrochim. Acta Part A* **62**, 97–104 (2005).

277. D. L. Howard and H. G. Kjaergaard, Influence of intramolecular hydrogen bond strength on OH-stretching overtones. *J. Phys. Chem. A* **110**, 10245–10250 (2006).

278. D. Christen and H. S. P. Müller, The millimeter wave spectrum of aGg' ethylene glycol: The quest for higher precision. *Phys. Chem. Chem. Phys.* **5**, 3600–3605 (2003).

279. D. P. Geerke and W. F. Van Gunsteren, The performance of non-polarizable and polarizable force-field parameter sets for ethylene glycol in molecular dynamics simulations of the pure liquid and its aqueous mixtures. *Mol. Phys.* **105**, 1861–1881 (2007).

280. R. Chelli, F. L. Gervasio, C. Gellini, P. Procacci, G. Cardini, and V. Schettino, Density functional calculation of structural and vibrational properties of glycerol. *J. Phys. Chem. A* **104**, 5351–5357 (2000).

281. C. S. Callam, S. J. Singer, T. L. Lowary, and C. M. Hadad, Computational analysis of the potential energy surfaces of glycerol in the gas and aqueous phases: Effects of level of theory, basis set, and solvation on strongly intramolecularly hydrogen-bonded systems. *J. Am. Chem. Soc.* **123**, 11743–11754 (2001).

282. G. Maccaferri, W. Caminati, and P. G. Favero, Free jet investigation of the rotational spectrum of glycerol. *J. Chem. Soc. Faraday Trans.* **93**, 4115–4117 (1997).

283. M. Jetzki, D. Luckhaus, and R. Signorell, Fermi resonance and conformation in glycolaldehyde particles. *Can. J. Chem.* **82**, 915–924 (2004).

284. M. Jetzki and R. Signorell, The competition between hydrogen bonding and chemical change in carbohydrate nanoparticles. *J. Chem. Phys.* **117**, 8063–8073 (2002).

285. R. A. Jokusch, F. O. Talbot, and J. P. Simons, Sugars in the gas phase—Part 2: The spectroscopy and structure of jet-cooled phenyl β-D-galactopyranoside. *Phys. Chem. Chem. Phys.* **5**, 1502–1507 (2003).

286. E. C. Stanca-Kaposta, D. P. Gamblin, J. Screen, B. Liu, L. C. Snoek, B. G. Davis, and J. P. Simons, Carbohydrate molecular recognition: A spectroscopic investigation of carbohydrate-aromatic interactions. *Phys. Chem. Chem. Phys.* **9**, 4444–4451 (2007).

287. R. Signorell, M. K. Kunzmann, and M. A. Suhm, FTIR investigation of non-volatile molecular nanoparticles. *Chem. Phys. Lett.* **329**, 52–60 (2000).

288. G. Firanescu, D. Hermsdorf, R. Ueberschaer, and R. Signorell, Large molecular aggregates: From atmospheric aerosols to drug nanoparticles. *Phys. Chem. Chem. Phys.* **8**, 4149–4165 (2006).

289. M. Quack and M. A. Suhm, Spectroscopy and quantum dynamics of hydrogen fluoride clusters, in *Molecular Clusters*, Advances in Molecular Vibrations and Collision Dynamics, Vol. III, J. M. Bowman and Z. Bačić, eds., JAI Press, London, 1998, pp. 205–248.

290. M. Quack, Spectra and dynamics of coupled vibrations in polyatomic molecules. *Annu. Rev. Phys. Chem.* **41**, 839–874 (1990).

291. T. Scharge, T. N. Wassermann, M. A. Suhm, Weak hydrogen bonds make a difference: Dimers of jet-cooled halogenated ethanols. *Z. Phys. Chem.* **222**, 1407–1452 (2008).